Missouri S&T Library and Learning Resources

Scholars' Mine

Masters Theses

Student Theses and Dissertations

Fall 2010

The properties and structure of tin phosphate glasses modified with other oxides

Jong Wook (Austin) Lim

Follow this and additional works at: https://scholarsmine.mst.edu/masters_theses

 Part of the Ceramic Materials Commons

Department:

Recommended Citation

Lim, Jong Wook (Austin), "The properties and structure of tin phosphate glasses modified with other oxides" (2010). *Masters Theses*. 6787.
https://scholarsmine.mst.edu/masters_theses/6787

This thesis is brought to you by Scholars' Mine, a service of the Missouri S&T Library and Learning Resources. This work is protected by U. S. Copyright Law. Unauthorized use including reproduction for redistribution requires the permission of the copyright holder. For more information, please contact scholarsmine@mst.edu.

THE PROPERTIES AND STRUCTURE OF TIN PHOSPHATE GLASSES MODIFIED WITH OTHER OXIDES

by

JONG WOOK (AUSTIN) LIM

A THESIS

Presented to the Faculty of the Graduate School of the

MISSOURI UNIVERSITY OF SCIENCE AND TECHNOLOGY

In Partial Fulfillment of the Requirements for the Degree

MASTER OF SCIENCE IN CERAMIC ENGINEERING

2010

Approved by

Dr. Richard K. Brow, Advisor

Dr. Delbert E. Day

Dr. Matt O'Keefe

PUBLICATION THESIS OPTION

This thesis has been prepared in the style utilized by the Journal of Non-Crystalline Solids. The paper I (pages 5-25) will be submitted for publication in that journal. The paper II (pages 26-50) was published in the Journal of Non-Crystalline Solid. Paper III (pages 51-70) will be prepared and submitted for publication in that journal. Appendices A and B have been added for purposes normal to thesis writing.

ABSTRACT

The main objective of this research was to evaluate the properties and structures of glasses from the stannous (SnO) phosphate system for possible use in low temperature optical applications. Glasses in the binary $xSnO\text{-}(100\text{-}x)P_2O_5$ system ($50 \leq x \leq 70$) were prepared and their thermal and optical properties were evaluated. Differences in glass transition temperatures (T_g) measured here and reported in the literature were explained by differences in the residual water content in the glasses, as determined by infrared spectroscopy. In general, increasing the SnO content of the binary glasses increased the refractive index and the glass transition temperature, and reduced the residual water content, producing glasses that are more chemically stable. Raman spectroscopy showed that the chain-length of the average phosphate anion decreased with increasing SnO content. The addition of B_2O_3 to a Sn(II)-pyrophosphate base glass (x= 67) improves the aqueous dissolution rate by an order of magnitude. The impact of these compositional changes on the optical and thermal properties depends on how the borate is added. Raman and nuclear magnetic resonance spectroscopies reveal that boron is initially incorporated into the glass network in tetrahedral sites and the pyrophosphate anions are converted to orthophosphate anions. The effects of the addition of Ga_2O_3 and Sb_2O_3 on the properties of the tin phosphate glasses were also determined. In general, the addition of these modifying oxides increase the glass transition temperature from around 250°C to 350°C, and the refractive index (n_D) was in the range 1.75-1.85, depending on glass composition. The chemical durability of these modified glasses was similar to those modified by B_2O_3-additions. Raman spectroscopy revealed the formation of isolated orthophosphate anions in the formation of Ga (Sb)-O-P glass networks.

ACKNOWLEDGEMENTS

I would like to express my gratitude to my advisor, Dr. Richard K. Brow, for his support and guidance to help me pass through difficult times and to finish my graduate studies. I have received and have benefited from his knowledge and understanding of glass science everywhere.

I express my thanks to Dr. S. W. Yung, National United University (Miao-Li, ROC), who provided me guidance for my research and my thanks to Dr. C. S. Kim for providing and sharing his experience and his prism coupler for my research.

I really appreciate Dr. Mariano Velez and Rex Carnes from Mo-Sci Co. for allowing me to use their lab spaces and for providing me their support and knowledge of the measurement of refractive index.

I would like to thank our professors in the Department of Materials Science and Engineering for the great educational experience that I had. I also express my thanks to Dr. Eric Bohannon and Dr. Elizabeth Kulp for their help and advice in the lab. I thank the MRC staff and technicians for their support of my work.

I am grateful and give thanks to all my research group colleagues (graduate and undergraduate) and other graduate students in MSE, including Signo, Nate, Melodie, Harlan, Chris, Sagnik, Rick, Zhongzhi, Jamie, Lina, Xiaoming, Char, Katie, and others who have helped me in one way or another.

I would like to thank my family and my friends, especially my wife, Ji Woo Park (Helena), for her love, understanding, patience and trust. She has always been there for me with her encouragement and support during my studies. Their love and trust have encouraged me to accomplish my goal.

TABLE OF CONTENTS

LIST OF ILLUSTRATIONS

Page

SECTION 1

PAPER I

PAPER II

LIST OF TABLES

Page

SECTION

1. INTRODUCTION

Aspherical lenses are becoming increasingly popular for a wide variety of applications, including the digital optical systems found in camera cell phones, ultra-thin digital cameras, and medical devices. An aspherical lens provides the solution for image distortion and spherical aberration and the use of glass aspherical elements has increased steadily in order to meet the demand of cheaper, better, lighter, and smaller optical devices. A survey from the Industrial Technology Research Institute in 2007 indicates that over 300 million of these lenses were produced in 2006 [1].

In the past decade, spherical lenses have used for most lens devices. These lenses are simple to produce using mass-manufacturing techniques, but are space consuming because it is necessary to use multiple lenses to eliminate the spherical aberration problem as shown in Figure 1.1 (a). These limitations can be compensated by using the aspherical lens with ideal curved surface as shown in Figure 1.1 (b). As shown in Figure 1.2, aspherical elements can optimize the focus of edge and center light rays, but it is difficult to produce the delicate curved surface and time consuming for a skilled technician to manually polish lenses one by one. The overall costs of polishing are very high for medium to high volume production of aspherical lenses [4-5]. In addition, there are environmental concerns due to the use of cutting fluids and health hazards associated with glass debris, particularly for glasses having high lead concentrations. Precision molding of aspherical lens is an attractive approach [6-7] and this method can significantly reduce the processing difficulties associated with polishing glasses.

Figure 1.1. (a) Distorted image from spherical lens. (b) Distortion free image with the help of aspherical lens [2].

Researchers are now trying to develop glass systems with the requisite thermal and optical properties for use in the glass molding process.

For the precision molding technique, glass is reheated above the softening temperature in a press mold to form the final desired shape [8]. This press molding operation is currently done at 700°C but the mold materials deteriorate under these conditions. Therefore, there is a desire for researchers to develop optical glasses with lower softening temperature (<500°C) that will extend the lifetimes of the very expensive precision optical molds. In addition, the new low temperature glasses must exhibit good chemical stability because low melting glasses often have poor chemical stability and their hygroscopic characteristics make them impractical for commercial applications.

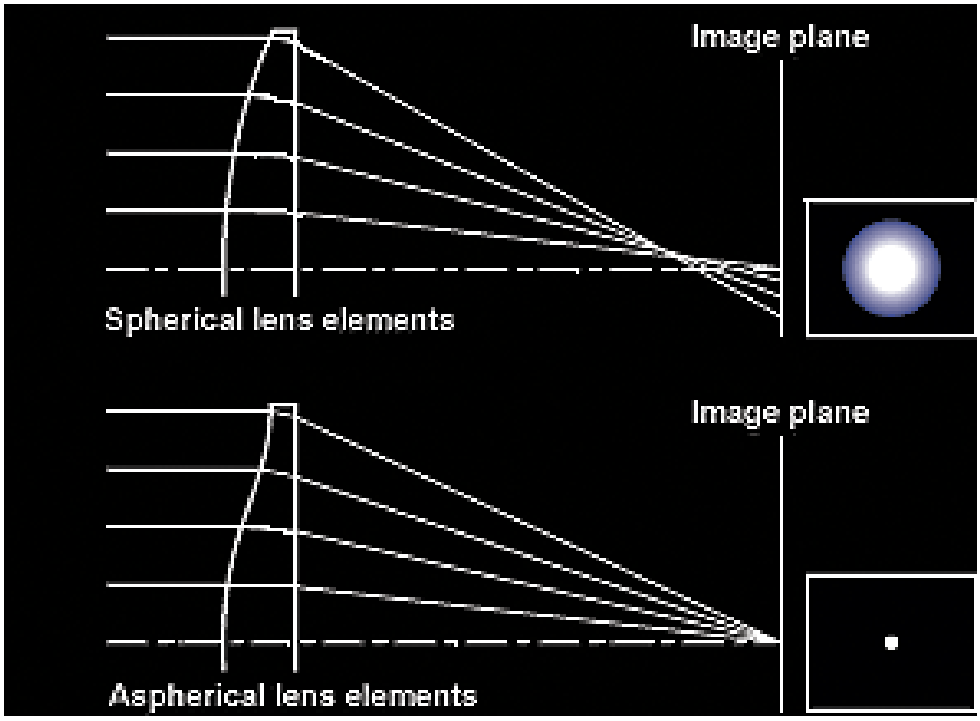

Figure 1.2. Aspherical lens by changing the shape of spherical lens can compensate for the spherical aberration [3].

The optical properties of glasses which are used for aspherical lenses include transparency through the visible range with high refractive indices (n_d>1.7), and relatively low dispersion (defined by an Abbe number, ν_d>20, where $\nu_d = (n_d-1)/(n_f-n_c)$ and n_d, n_f, and n_c are refractive indices measured at 486.1, 589.3, and 656.3nm, respectively). These optical properties must be retained during the molding process of aspherical lenses.

Phosphate based glasses have been developed with the range of optical, thermal, and chemical properties for precision press molded optical lenses [9-11]. These glasses contain 20~40 mol% P_2O_5 and are modified by high index oxides such as Nb_2O_5, Ta_2O_5, Bi_2O_3, and La_2O_3 to produce the desired optical properties (n_d > 1.7); however, their softening temperatures are typically over 500°C. For example, P-SF67 glass developed

by Schott for press precision molding operations has a refractive index (n_d) of 1.9068, an Abbe number of 21.40, and a glass transition temperature (T_g) of 539°C [12]. Thus, there is an opportunity to develop new compositions with lower softening temperatures that could be molded at lower temperatures and still have high chemical resistivity and good optical characteristics.

The purpose of this thesis is to evaluate the properties and structures of stannous phosphate glasses for their potential use as low temperature optical glasses.

PAPER

I. PROPERTIES AND STRUCTURE OF BINARY TIN PHOSPHATE GLASSES

J.W. Lim [a], S.W. Yung [b] and R.K. Brow [a]

[a] Missouri University of Science & Technology, Department of Materials Science & Engineering, Rolla, MO 65409 USA

[b] National United University, Department of Materials Science & Engineering, Miao-Li 36003, Taiwan, ROC

ABSTRACT

The properties and structure of binary $xSnO*(100-x)P_2O_5$ ($50 \leq x \leq 70$) glasses are reported. The glasses were prepared in vitreous carbon crucibles by melting under argon at 1000°C. The glass transition temperatures, determined by differential thermal analysis (DTA), range from 246 to 264°C. The refractive index (n_D) increases from 1.701 to 1.833 as x increases from 50 to 70, and the Abbe number (ν_D) decreases from 29.1 to 20.4 over the same range. Infrared spectroscopy was used to estimate water contents in the glasses, which decreased with an increase in SnO content, from about 1570 ppm OH for x=50 to about 50 ppm OH for x=70. Raman spectroscopy indicates that progressively shorter phosphate chains are present in the structures of the binary Sn-phosphate glasses with increasing SnO-contents.

1. INTRODUCTION

The Sn(II)O-P_2O_5 glass-forming system offers the possibility for the development of new low temperature glasses for packaging and optical applications. Previous low melting glasses often have PbO as a major component but Pb-free glass systems are preferred to avoid the deleterious health and environmental effects of lead [1]. SnO has been used to decrease the melting temperature and glass transition temperature of phosphate glasses [2]. These glasses have unusually low characteristic temperatures (glass transition temperatures under 300°C) and high refractive indices (n_D>1.7). Previously, Takebe, et al. [3] described a transparent glass with the nominal composition of 67SnO-33P_2O_5 (mole %), possessing a refractive index (n_D) of 1.794 and a glass transition temperature of 268°C. Ehrt [4] reports that a glass with the nominal composition 60SnO-40P_2O_5 (mole %) has a glass transition temperature of 300°C, an n_d of 1.762 and an Abbe number (ν_d) of 26.7. Recently, the properties of tin pyrophosphate glasses modified with B_2O_3 have been reported [5]. Chemically-durable stannous borophosphate (SBP) compositions with refractive indices >1.78 and glass transition temperatures <300ºC were identified.

There are several recent reports on the properties and structure of binary Sn(II)O-P_2O_5 glasses, but the data is inconsistent [3-4, 6-8], due in part to differences in raw materials and melting conditions used to prepare the glasses. For example, Ehrt [4] has shown that the glass transition temperature of a glass with the nominal molar composition 60SnO-40P_2O_5 can vary by 100°C depending on melting conditions, due to a difference in the amount of residual water that can be incorporated into the glass structure, and due to the possible oxidation of Sn(II) to Sn(IV).

In the present study, thermal and optical properties of binary SnO-phosphate glasses are reported. Water contents are estimated from infrared absorption analyses and are used to account for differences in properties from similar glasses described in the literature. Information about the nature of the phosphate anions that constitute the glass structure is provided by Raman spectroscopy.

2. EXPERIMENTAL METHOD

2.1 GLASS PREPARATION

Binary glasses in the compositional range for $xSnO*(100-x)\ P_2O_5$ ($50 \leq x \leq 70$) were prepared from reagent grade $Sn_2P_2O_7$ (Alfa Aesar), SnO (Alfa Aesar, 99.9%), and P_2O_5 (Alfa Aesar, 99.99%). After thoroughly mixing the components in a nitrogen glove box, the batch was preheated at 600°C for 20 minutes and then melted for 15 minutes at 1000°C in a vitreous carbon crucible in a silica tube furnace under flowing argon in order to avoid oxidation of Sn^{2+} to Sn^{4+}. The homogeneous melts were quenched on copper plates in air and annealed for 3 hours between 230 and 270°C, depending on composition.

2.2 CHARACTERIZATION

Differential thermal analysis (DTA 7, Perkin Elmer) was used to determine the glass transition temperature (T_g). About 40 mg of sample powder (particle size 425~500 μm) was heated at 10°C/min in an alumina crucible under nitrogen. Onset temperatures were determined using the tangent method and the estimated uncertainty of these characteristic temperatures is $\pm$ 3°C. The density was measured by the Archimedes method with distilled water or kerosene as the buoyancy fluid. Four samples of each

glass composition were measured and the standard deviation is used as the error (typically ±0.005 g/cm^3).

Optical transmission measurements were made using a Cary 5 UV-Vis-NIR spectrophotometer, on samples that were 0.6-0.8 mm thick and polished to 1μm (diamond paste). The UV edge was taken as the wavelength at which absorbance equals 1 cm^{-1} [9]. The refractive indices of these polished samples were measured using a prism coupling technique (Metricon 2010) with laser sources at 405, 632.8, and 785 nm; the uncertainty of these measurements is ±0.0002. An Abbe number, $\nu_D=(n_D-1)/(n_F-n_C)$, was determined by calculating refractive indices at 656.3 nm (n_C), 589.3 nm (n_D) and 486.1 nm (n_F) after fitting the three measured refractive indices using the Cauchy dispersion equation:

$$n(\lambda) = a + b*\lambda^{-2} + c*\lambda^{-4} \text{ (where } \lambda \text{ is wavelength)}$$

The infrared absorption measurements were recorded using a Fourier transform infrared spectrometer (Thermo Nicolet Nexus 670). Polished samples with various thicknesses between ~ 0.5 to 1 mm were analyzed in the wavenumber range from 400 to 4000 cm^{-1} and the absorption band in the range 2800-3200 cm^{-1} was used to estimate the residual water contents in the glasses.

A chemical analysis of the glasses was obtained by X-ray fluorescence spectrometry. About 0.5 g of powder from each sample was obtained by grinding the samples in a mortar and pestle; the powders were pressed into a disk about 32 mm in diameter and analyzed using a Spectro Xepos-EDXRF spectrometer. The spectra were

analyzed using software provided by the spectrometer manufacturer and the compositional accuracy is ± 10~20% relative.

Raman spectra were collected on each bulk glass using a Jobin-Yvon micro-Raman spectrometer (LabRAM ARAMIS) with a 632.8 nm He-Ne laser as the excitation source. The samples were scanned for 5 seconds and resolution was 50x magnifications.

3. RESULTS

3.1 GLASS FORMATION AND PROPERTIES

Homogeneous glasses from melts from the SnO-P_2O_5 (SP) glass system were quenched with nominal compositions from 50 mol% to 70 mol% SnO. Samples typically lost less than 2% of their expected mass after melting, indicating that the final glass compositions do not differ significantly from the 'as batched' compositions. With the addition of SnO, the glasses became noticeably less hydroscopic.

Table 1 summarizes the XRF analyses and selected properties of the tin phosphate glasses. In general, the analyzed SnO contents are in agreement with the batched compositions, within the uncertainties of the XRF analyses. The systematic compositional dependence of properties, like the refractive index and density in Table 1, indicates that the glass compositions do not vary in the manner suggested by the XRF results. For this reason, the batched compositions will be used to describe the compositional and structural trends.

Figure 1 compares the glass transition temperature from the present study with values reported in the literatures [3-4, 6-8]. In the present study, T_g decreases with an increase in SnO-content from 50 to 55 mole%, then increases with further increases in

SnO-content. A similar trend has been noted for the glass transition temperatures of binary ZnO-phosphate glasses over the same compositional range [10]. There is good agreement between the values of T_g determined here and reported by Cha, et al. [7] and Takebe et al. [3], whereas those reported by Moringa et al. [6] are 50-100°C lower than our data, and the value of T_g for a glass with 60 mole% SnO reported by Ehrt [4] is about 50°C greater than the comparable glass in this study. The refractive indices (at 589 nm) of the glasses determined in this study are in good agreement with those reported by others [3-4, 7], with a systematic increase in refractive index with increasing SnO-content (Figure 2). Figure 3(a) shows a similar compositional dependence for the glass density, which was then used with the nominal glass composition to calculated the molar volumes shown in Figure 3(b); the latter decrease systematically with increasing SnO content. Figure 4 shows that the UV edge shifts to longer wavelengths with increasing SnO content. The data in the present study are in good agreement with that reported by Cha *et al.* [7].

3.2 SPECTROSCOPIC STUDIES

Figure 5 shows the infrared absorption spectra from the SnO-P_2O_5 glasses. The absorption peak in the range 2800~3100 cm^{-1} is due to the symmetric stretching mode of O-H species incorporated in the glass structure [11]. The intensity of the peak decreases and the position of the peak shifts to higher frequency as the SnO content of the glass increases. According to Efimov et al. [11], the band at 2837cm^{-1} can be related only to the asymmetric vibrational mode of the H_2O molecule, whereas the bands at 3175 and

3410cm^{-1} can be related to either the stretching mode of the "free" P-O-H group or the symmetric vibrational mode f the H_2O molecule.

The extinction coefficient for this band has been reported to be 90~100 ppm OH per cm^{-1} [12-13], and these values were used to estimate the residual water content of the glasses, as summarized in Table 2. For glasses melted at 1000°C and 15 minutes, the residual OH content decreases from about 1500 ppm for the 50SnO glass to about 50 ppm for the 70SnO glass, with an uncertainty of about ±20%. The OH content in the 50SnO glass is equivalent to about 1 mol% H_2O. 50SnO glass and 60SnO glass have broad peaks in the range 2500~3500 cm^{-1}.

Raman spectra from the SnO-P_2O_5 glasses are shown in Figure 6. The bands near 1170 cm^{-1} are assigned to the symmetric stretching modes associated with P-nonbridging oxygens on tetrahedra that link two neighboring tetrahedra through bridging oxygens (Q^2) [10] and the bands at 1050cm^{-1} are due to the symmetric P-O stretch of nonbridging oxygens on tetrahedra that are linked to one other tetrahedron (Q^1). The bands at 950cm^{-1} are assigned to the P-O symmetric stretch of nonbridging oxygens on isolated (Q^0) tetrahedra. The bands between 650 and 775 cm^{-1} are assigned to P-O-P stretching modes, and the shift to higher frequencies with greater SnO content has been noted for other series of phosphate glasses [14].

4. DISCUSSION

The properties of the binary SnO phosphate glasses change systematically with composition. In particular, density (Figure 3(a)) and refractive index (Figure2) increase with increasing SnO content. These trends are expected given the relative atomic mass of

Sn (118.71 amu) compared to P (30.97 amu). In addition, the systematic decrease in the molar volumes of the glasses with increasing SnO content (Figure 3(b)) may also contribute to the positive trends in density and refractive index. The reduction in the molar fraction of oxygen ions in a glass as SnO replaces P_2O_5 will contribute to the systematic decrease in glass molar volume since the size of an oxygen ion exceeds that of both Sn^{2+} and P^{5+}.

The shift of the UV edge to longer wavelengths with increasing SnO content (Figure 4) is the result of the electronic transitions associated with the $5s^2$ electronic configuration of the Sn^{2+} ions [4]. The higher concentrations of SnO increase the probability for the relevant $S \rightarrow P$ transitions, and the red-shift in the UV edge is consistent with the decrease in Abbe number (Table 1) with increasing SnO content.

The compositional dependence of the glass transition temperature (Figure 1) is interesting. First, the glass transition temperatures of the SnO phosphate glasses are low, about 100°C lower than comparable PbO phosphate glasses and about 200°C lower than comparable ZnO phosphate glasses [10]. The low processing temperatures for these glasses make them potential candidates for a variety of optical and sealing applications. Next, T_g generally increases with increasing SnO content, particularly above 60 mol% SnO. This may reflect somewhat stronger Sn-O bonds replacing P-O bonds in the glass structure, and the denser packing (lower molar volume) of glass structures with increasing SnO content.

Of the various properties measured in this study, there is the greatest variation in the values of T_g reported by different researchers (Figure 1), and this is most likely due to variations of the residual water content in the different glasses. For example, Ehrt [4]

describes two glasses with the same nominal $60SnO{\cdot}40P_2O_5$ composition. One glass, melted for 30 minutes at a 450°C had about 3.5 wt% OH and a T_g of 200°C, whereas a glass melted for 2 hours at a 1200°C had about 0.01 wt% OH and a T_g of 350°C. As shown in Figure 1, Morinaga et al. [6] had 50~140°C lower T_g than other reported data. They did not report the OH content of their glasses but their glasses were melted at 500°C for 5 min in air and so are expected to possess relatively large content of residual water, the incorporation of which will decrease the T_g of phosphate glasses [15].

The Sn^{2+} ion possess an electron lone pair that affects the coordination environment of tin polyhedra. For example, the tin lone pair has been proposed to form the apex of trigonal SnO_3 pyramids in phosphate glasses [16-17]. The lack of strong bonding cross links through this corner of the Sn-polyhedron contributes to the relatively low glass transition temperatures associated with the SnO glasses.

The nature of the phosphate anions that constitute the other part of the glass structure changes systematically with SnO content. The Raman spectra in Figure 6 indicate that the phosphate tetrahedral units systemically convert from Q^2 to Q^1 units as the SnO content increases from 50 mole% to 70 mole%. The intensity of the 1170 cm^{-1} bands become weaker as the SnO content increases and the intensity of the peak at 1050 cm^{-1} increases. Above about 60 mol% SnO, the intensity of the Q^0 peak near 950 cm^{-1} increases so that the spectrum of the 70SnO glass reveals a structure based on Q^1 and Q^0 units. The compositional dependence of the peak near 700 cm^{-1}, due to P-O-P symmetric stretching modes, is consistent with the evolution of the phosphate network from one dominated by Q^2 units that link neighboring phosphate tetrahedra in relatively large anions at 50SnO (693 cm^{-1}), to one dominated by Q^1 tetrahedra that terminate relatively

small phosphate anions at 70SnO (743 cm^{-1}). This interpretation is consistent with the conclusions of previous Raman [7-8] and NMR [14, 18-19] studies of SnO phosphate glasses.

5. CONCLUSION

Binary tin phosphate glasses with 50~ 70 SnO mol% were prepared and their structure and properties were investigated. The addition of SnO to the binary system increased the glass transition temperature and refractive index. Raman spectra indicate that the formation of covalent Sn-O-P bonds from P-O-P network produces a stronger, more packed network. Further additions of SnO produce more complex phosphate (Q^1 and Q^0) tetrahedra units. The glass transition temperature is affected by the OH content in glass and OH content increases the number of weak bonds in the glass network, reducing T_g.

ACKNOWLEDGEMENTS

The authors thank Tamara Weimer and Mariano Velez (Mo Sci) for collecting the XRF data and Curtis Planje (Brewer Science) for helping with the refractive index measurements. The financial support of the Government of the Republic of China (project No. 97-EC-17-A-08-S1-033) is gratefully acknowledged.

REFERENCES

[1] US Federal Registry, 44 (1979) 60980-60994.

[2] R. Morena, J. Non-Cryst. Solids, 263-264 (2000) 382.

[3] H. Takebe, W. Nonaka, T. Kubo, J. Cha, and M. Kuwabara, J. Phys. Chem. Solids, 68 (2007) 983-86.

[4] D. Ehrt, J. Non-Cryst. Solids, 354 (2008) 546-552.

[5] J. W. Lim, M. L. Schmitt, S. W. Yung, and R. K. Brow, J. Non-Cryst. Solids, 356 (2010) 1379-1384.

[6] K. Morinaga and S. Fujino, J. Non-Cryst. Solids, 282 (2001) 118-124.

[7] J. Cha, T. Kubo, H. Takebe, and M. Kuwabara, J. Ceram. Soc. Japan, 116 [8] (2008) 915-919.

[8] A. Hayashi, T. Konishi, K. Tadanaga, T. Minami and M. Tatsumisago, J. Non-Cryst. Solids, 345&346 (2004) 478-483.

[9] J. E. Shelby, J. Am. Ceram. Soc., 71 [5] (1988) C254-256.

[10] R. K. Brow, D.R. Tallant, S.T. Myers, and C.C. Phifer, J. Non-Cryst. Solids, 191 (1995) 45-55.

[11] A.M. Efimov, R. G. Kostyreva, G.A. Sycheva, J. Non-Cryst. Solids, 238 (1998) 124-142.

[12] H. Ebendorff-Heidepriem, W. Seeber, and D. Ehrt, J. Non-Cryst. Solids, 163 (1993) 74.

[13] P.R. Ehrmann, K. Carlson, J.H. Campbell, C.A. Click, and R.K. Brow, J. Non-Cryst. Solids, 349 (2004) 105-114.

[14] J. J. Hudgens, R. K. Brow, D. R. Tallant, and S.W. Martin, J. Non. Cryst. Solids, 223[1,2] (1998) 21-31.

[15] J. J. Hudgens and S.W. Martin, J. Am. Ceram. Soc., 76 [7] (1993) 1691-1696.

[16] R. K. Brow, C.C. Phifer, X.J. Xu, and D.E. Day, Phys. Chem. Glasses 30 (1992) 33.

[17] D. Holland, S.P. howes, M.E. Smith, and A.C. Hannon, J. Phys.:Condens. Matter 14 (2002) 13609.

[18] A. Hayashi, M. Nakai, M. Tatsumisago, T. Minami, Y. Himei, Y. Miura, and M. Katada, J. Non-Cryst. Solids, 306 (2002) 227-37.

[19] E. Bekaert, L. Montagne, L. Delevoye, G. Palavit, and B. Revel, C.R. Chimie 7 (2004) 377.

Table 1: Selected properties of the tin phosphate glasses.

SnO	XRF SnO	Density (±0.002)	Refrac. Index (±0.0003)	Glass Trans. (± 5°C)	UV-edge (± 1)	Abbe #
Mole%	Mole %	g/cm^3	(589.3 nm)	T_g (°C)	nm	ν_D
50.0	47	3.507	1.7008	246	299	29.08
55.0	48	3.6313	1.722	234	303	27.33
60.0	59	3.763	1.7486	241	310	24.66
65.0	65	3.9044	1.7794	256	318	23.33
70.0	63	4.1171	1.8332	265	331	20.40

Table 2: Observed OH infrared peak position and water content.

SnO (Mole%)	OH Peak Position (cm^{-1})	Est. Water Content (ppm OH)
50.0	2842	1569
60.0	2848	754
65.0	3074	146
70.0	3089	50

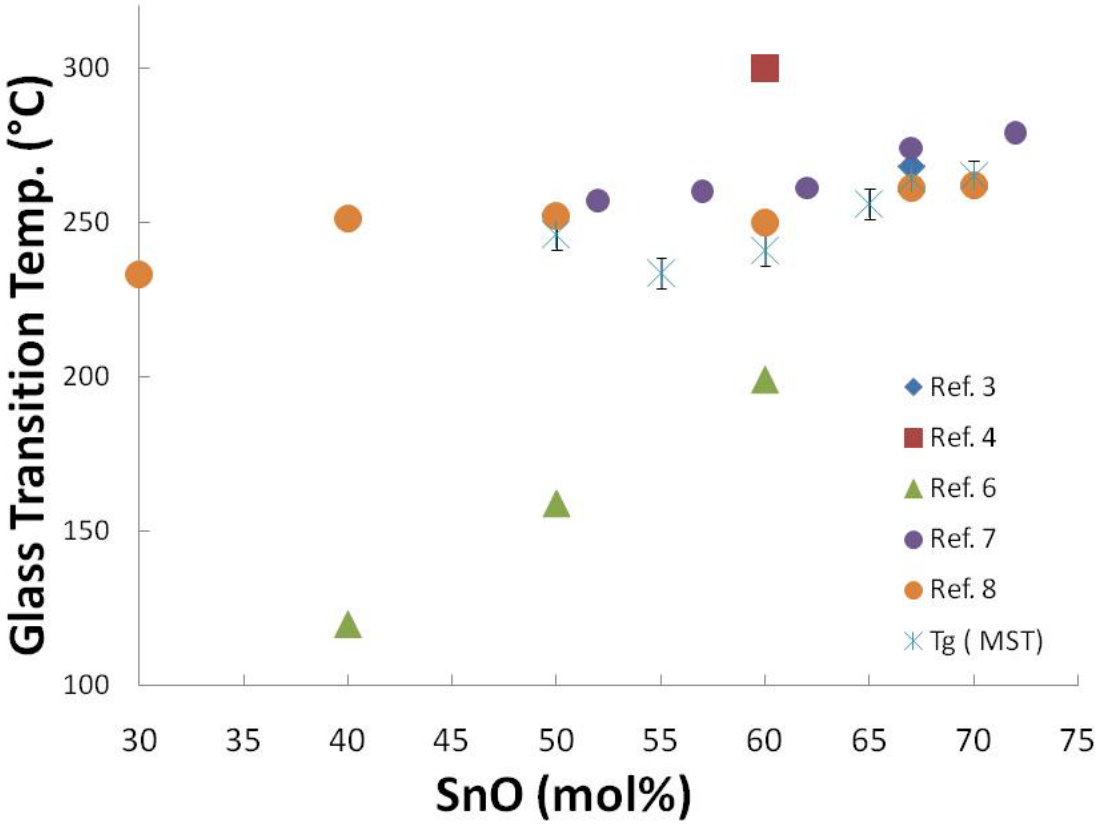

Figure 1. Glass transition temperature of tin phosphate glasses measured here and reported in the literatures.

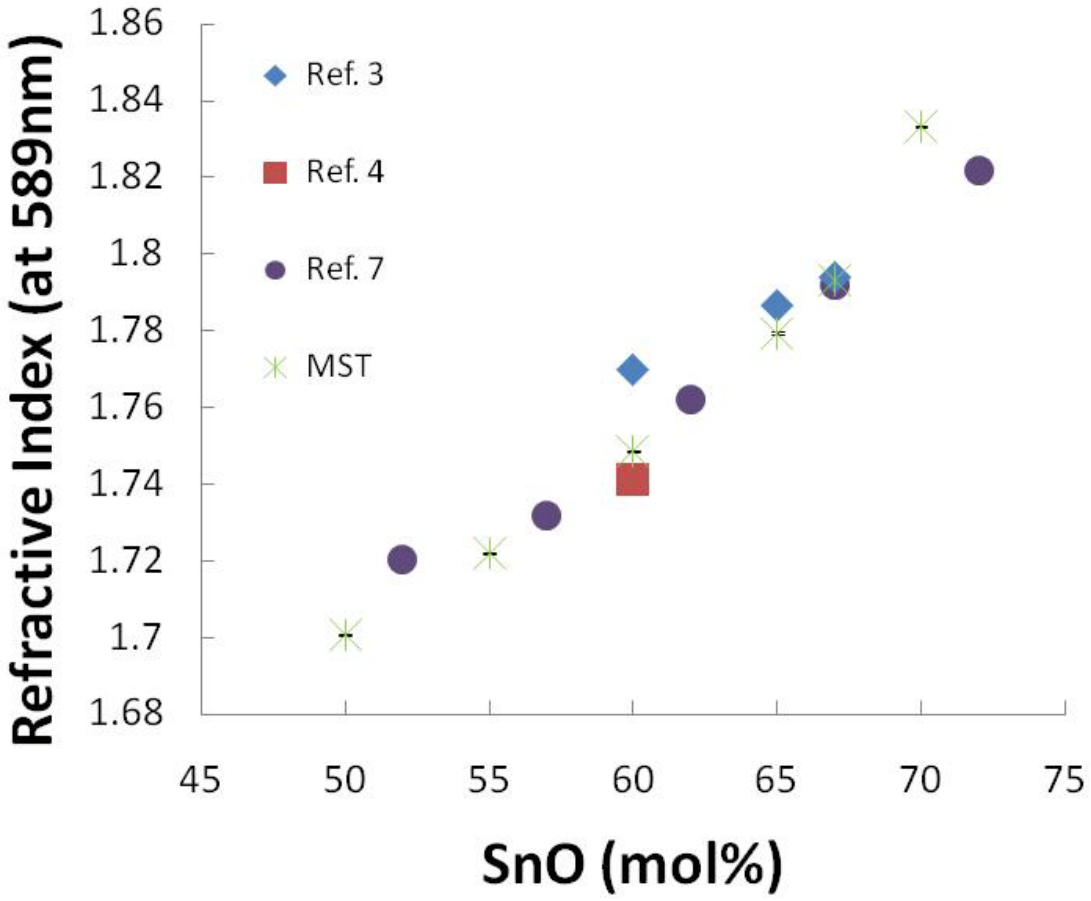

Figure 2. Refractive index of tin phosphate glasses measured here and reported in the literatures.

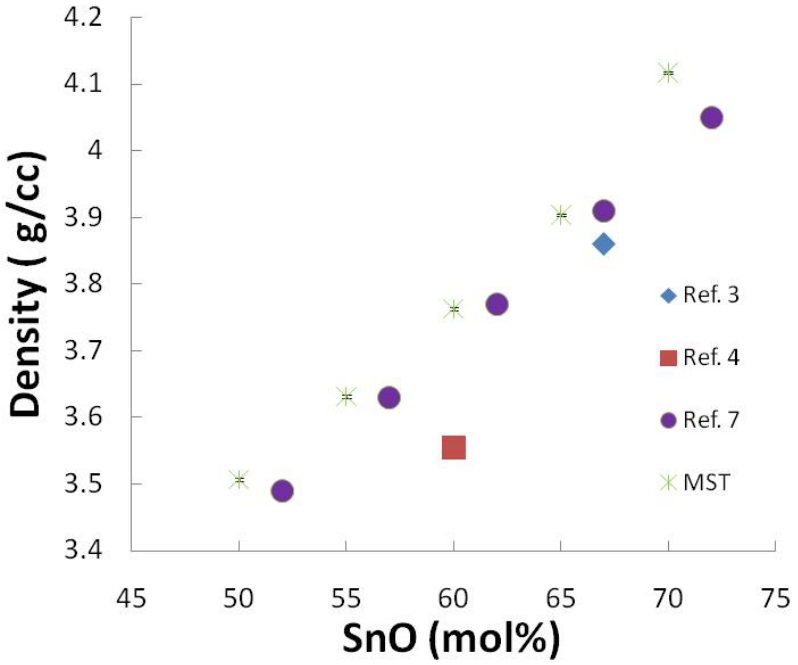

(a)

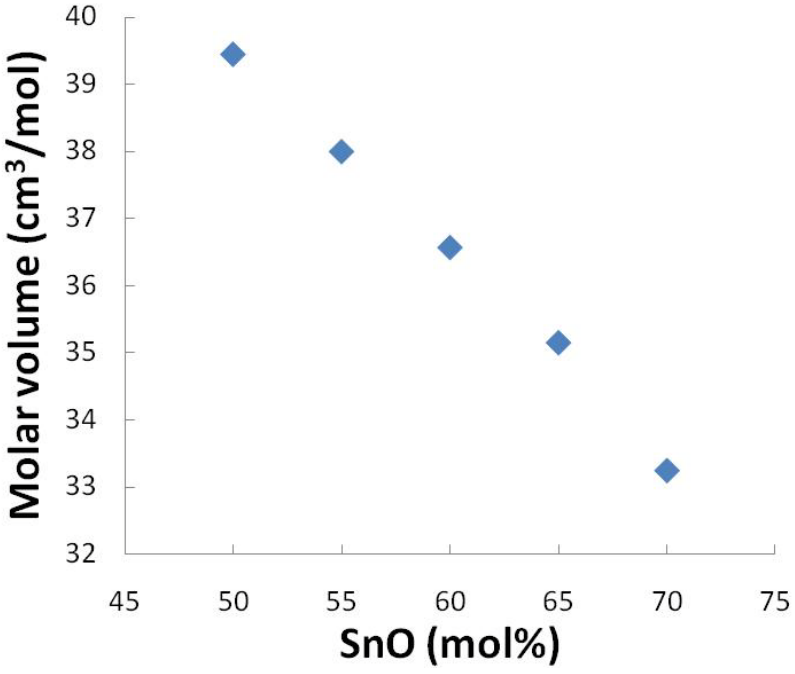

(b)

Figure 3. (a) Density of $SnO-P_2O_5$ glass measured here and reported in the literatures, (b) molar volume of the $SnO-P_2O_5$ glasses prepared in this study.

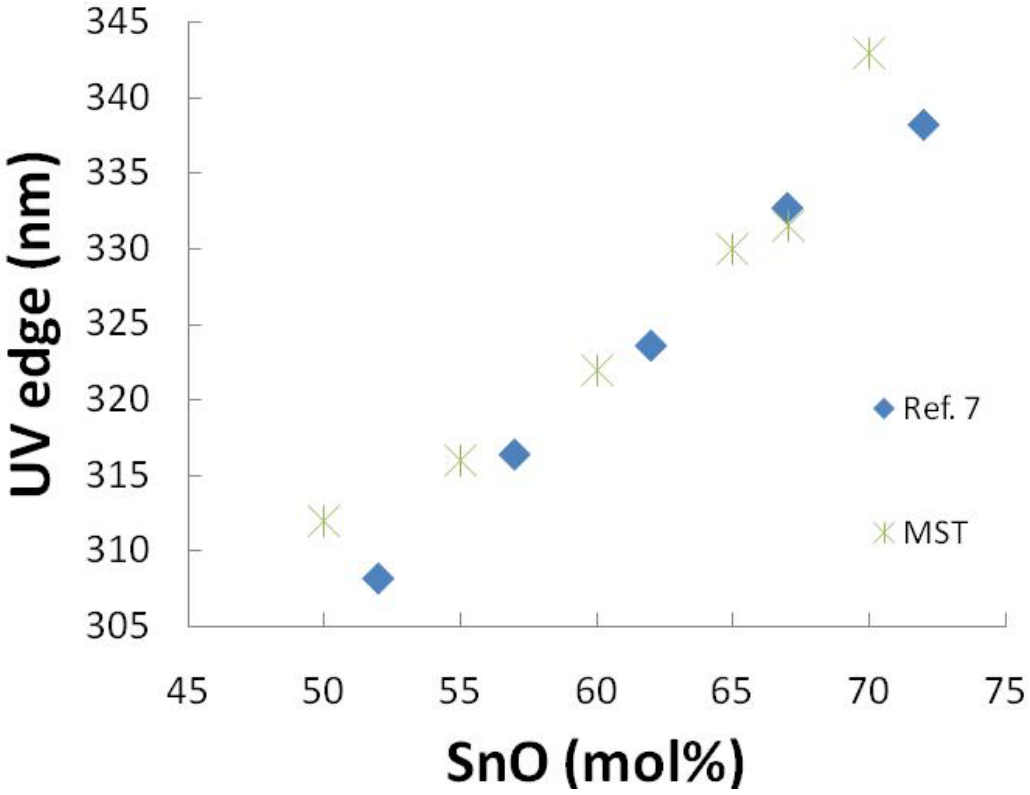

Figure 4. UV edge of tin phosphate glasses measured here and reported in the literature.

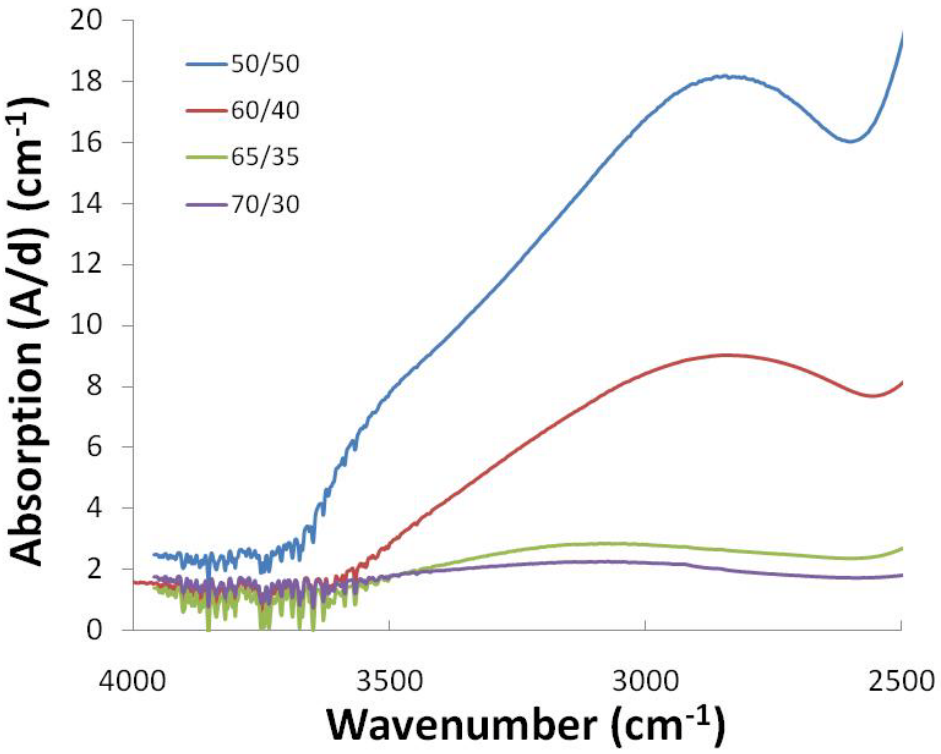

Figure 5. Infrared absorption spectra of the tin phosphate glasses.

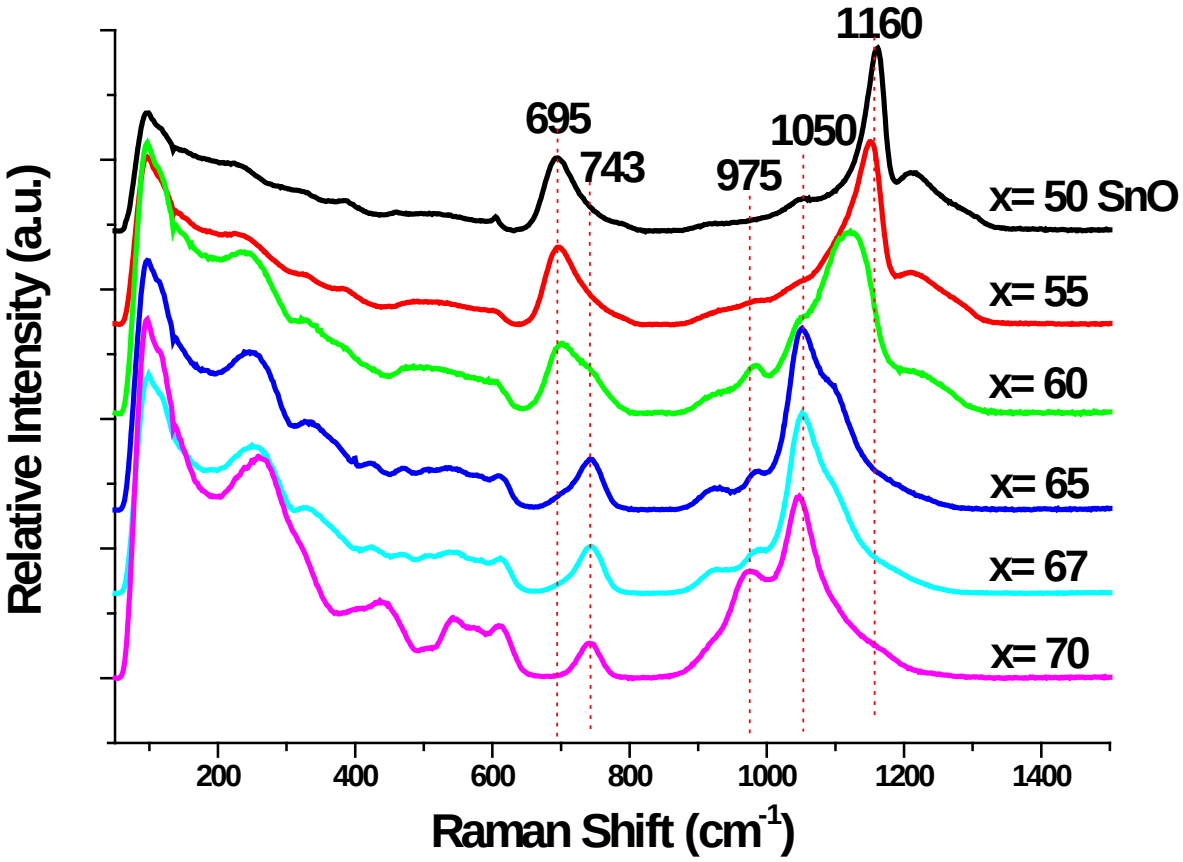

Figure 6. Raman spectra of $SnO\text{-}P_2O_5$ (SP) glasses.

II. PROPERTIES AND STRUCTURES OF TIN BOROPHOSPHATE GLASSES

J.W. Lim, M.L. Schmitt and R.K. Brow[1]

Missouri University of Science & Technology

Department of Materials Science & Engineering

Rolla, MO 65409 USA

S.W. Yang

National United University

Department of Materials Science & Engineering

Miao-Li 36003, Taiwan, ROC

[1] Corresponding author: brow@mst.edu

ABSTRACT

The effects of B_2O_3-additions on the properties and structures of two series of Sn(II)-borophosphate glasses were determined. The addition of up to 28 mole% B_2O_3 to a $66.7SnO{\cdot}33.3P_2O_5$ base glass (series I), and the substitution of up to 13 mole% B_2O_3 for P_2O_5 in the same base glass (series II) increase T_g from 265°C to 357°C and 306°C, respectively, while reducing the aqueous corrosion rates (at 40°C) by an order of magnitude. The refractive index of the series I glasses decreases slightly, from 1.784 to 1.725, and increase for series II, to 1.834, at 632.8 nm. Raman spectroscopy reveals that borate additions to both series reduce the number of P-O-P linkages by converting pyrophosphate anions to orthophosphate anions. ^{11}B NMR spectra indicate that tetrahedral borophosphate units, $B(OP)_4$, are initially formed when B_2O_3 is added to the Sn-pyrophosphate base glass. More complex tetrahedral and trigonal borate sites form when B_2O_3 contents exceed about 10 mole%.

1. INTRODUCTION

The Sn(II)O-P_2O_5 glass-forming system offers one possibility for developing new low temperature glasses for packaging and optical applications. The glasses have unusually low characteristic temperatures; glasses modified by SnF_2 have glass transition temperatures as low as 100°C [1-2]. The glasses are also characterized by good chemical durability. The combination of low characteristic temperatures and good chemical durability appears to be a consequence of the relatively weak bonds between tin polyhedra that are capped by unbonded electrons and the phosphate anions that make up the glass structure [3-4]. Chemically-stable Sn(II)-phosphate glasses have been developed for low-temperature sealing applications [5-7]. More recently, the optical properties of binary tin phosphate glasses have been reported. For example, Takebe, et al. [8] describe a transparent glass with the nominal composition of 67SnO-33P_2O_5 (mole%), possessing a refractive index (n_d) of 1.794 and a glass transition temperature of 268°C. Ehrt [9] reports that a glass with the nominal composition 60SnO-40P_2O_5 (mole%) has a glass transition temperature of 300°C, an n_d of 1.762 and an Abbe number (ν_d) of 26.7. Ehrt's data is consistent with Takebe's observation that n_d increases, and T_g decreases, with increasing SnO-content. SnO-phosphate and –borophosphate glasses have also been developed as anode materials for Li-batteries [10-11].

The addition of B_2O_3 to phosphate glasses is well-known to improve the chemical durability and affect other properties [12]. The thermal properties and chemical durabilities of Zn-borophosphate glasses have made them candidates for sealing applications and spectroscopic studies indicate that desirable properties result from the incorporation of tetrahedral borons in the glass network [13-15]. The replacement of

ZnO by SnO in simple phosphate glasses reduces the glass transition temperature, and the addition of B_2O_3 to SnO/ZnO-phosphate glasses improves their resistance to attack by water [16]. However, much less is known about the properties and structures of glasses in the ternary SnO-B_2O_3-P_2O_5 system. In this study, the properties and structures of two series of 66.7SnO-33.3P_2O_5 glasses modified by B_2O_3 are reported.

2. EXPERIMENTAL METHOD

2.1 GLASS PREPARATION

Two series of glass compositions were prepared from reagent grade SnO (Alfa Aesar, 99.9%), $Sn_2P_2O_7$ (Alfa Aesar), and H_3BO_3 (Fisher Scientific, 98%). In series I, B_2O_3 was added to a 66.7SnO·33.3P_2O_5 base glass according to xB_2O_3·(100-x) - (66.7SnO·33.3P_2O_5), and in series II, B_2O_3 replaced P_2O_5 in the base glass, according xB_2O_3·66.7SnO·(33.3-x)P_2O_5. Other compositions were prepared to determine the glass forming range. Batches that yielded 10g of glass were thoroughly mixed and then melted for 30 minutes at 900^{o}C in a vitreous carbon crucible in a silica tube furnace under flowing argon in order to avoid oxidation of Sn^{2+} to Sn^{4+}. The melts were quenched on copper plates in air and annealed between 260 and 360°C, depending on composition.

2.2 CHARACTERIZATION

Differential thermal analysis (DTA 7, Perkin Elmer) was used to determine glass transition (T_g) and crystallization temperatures (T_x). About 40 mg of sample powder (size 425~500 μm) was heated at 10°C/min in an alumina crucible under nitrogen. Onset temperatures were determined using the tangent method and the estimated uncertainties

of these characteristic temperatures is $\pm$ 3°C. The density was measured by the Archimedes method with distilled water as the buoyancy fluid. Four samples of each glass were measured and the standard deviation is used as the error (typically ±0.006 g/cm^3). Aqueous corrosion rates were determined from samples approximately 12mm x 6.5mm x 1mm, polished to 1 micron with a diamond suspension. The samples were suspended in 100 ml of distilled water (pH~6) in polypropylene containers held at 40°C. Samples were removed from the water at periodic intervals, dried in air for 20 minutes, and re-weighed to record weight losses. Corrosion rates reported here were determined after 24 hours on test.

Optical transmission measurements were made using a Cary 5 UV-Vis-NIR spectrophotometer, on samples that were 0.6-0.8 mm thick and polished to 1µm (diamond paste). The refractive indices of these polished samples were measured using a Metricon Refractometer at 632.8 nm; the uncertainty of these measurements is ±0.0002.

Raman spectra were collected from each glass using a Jobin-Yvon micro-Raman spectrometer with a 632.8 nm He-Ne laser as the excitation source. Solid state ^{11}B MAS-NMR spectra were recorded at 128.51 MHz on a Tecmag NMR spectrometer. A cylindrical silicon nitride (Si_3N_4) rotor with Torlon caps was rotated at a speed of 10 kHz and a recycle pulse delay of 1.0 s, and over 10,000 scans were collected for each spectrum.

3. RESULTS

3.1 GLASS FORMATION AND PROPERTIES

Clear, homogeneous glasses could be cast to thicknesses of 1 cm from series I melts at 900°C with up to 28 mole% B_2O_3 , whereas in series II, cast glasses with more than 10 mole% B_2O_3 were partially devitrified (Figure 1); clear glasses from series II with 13 and 16 mole% B_2O_3 were possible if the melt was quenched between copper blocks. Samples typically lost less than 1% of their expected mass after melting, indicating that the final glass compositions do not differ significantly from the 'as batched' compositions; therefore, the latter compositions are used in this report.

The DTA curves for series I and series II are shown in Figure 2(a) and 2(b), respectively. In both series, the addition of B_2O_3 increases the glass transition temperature (T_g) and reduces, then eliminates, the crystallization exotherm near 450-500°C that is apparent in the DTA curve from the $66.7SnO{\cdot}33.3P_2O_5$ base glass. Figure 3 summarizes the effects of composition on T_g.

The effects of glass composition on density are shown in Figure 4 (bottom). For series I, density decreases with B_2O_3-additions, whereas density increases with B_2O_3-additions in series II. The molar volumes, calculated from these densities and the respective nominal molecular weights, are also shown in Figure 4 (top); MV decreases systematically with increasing B_2O_3 contents for both series, but more significantly for series II. For series I, there appears to be a break in the compositional dependence of MV near 13 mole% B_2O_3. Figure 5 shows similar compositional dependencies for the refractive indices as were noted for density. B_2O_3 additions decrease the refractive index (at 632.8 nm) of glasses in series I, but increase the refractive indices of glasses in series

II. The refractive index of the $66.7SnO{\cdot}33.3P_2O_5$ base glass is in good agreement with the indices reported for similar compositions [8-9]. Figure 6 shows that the addition of 10 mole% B_2O_3 reduces the aqueous corrosion rate of both series of glasses by a factor of ~10.

Figure 7 shows optical transmission curves for several of the glasses, and the inset shows the compositional dependence of the UV edge. The glasses transmit well through the visible and near-infrared regions, to about 2700 nm. For series I, there is no obvious dependence of the UV-edge position on composition, whereas the wavelength of the edge increases systematically as B_2O_3 replaces P_2O_5 in series II.

3.2 SPECTROSCOPIC STUDIES

The Raman spectra from glasses in series I and II are shown in Figure 8(a) and 8(b), respectively. Peaks in the range of 600 to 1100 cm^{-1} can be assigned to vibrational modes associated with the phosphate network [17-18]. The spectrum from the $66.7SnO{\cdot}33.3P_2O_5$ base glass is comparable to what has been reported elsewhere for similar compositions [19], and is consistent with a glass structure dominated by pyrophosphate (Q^1) units. The intense band at 1050 cm^{-1} results from the symmetric P-O stretch of nonbridging oxygens on these Q^1 tetrahedra, and the sharp band at 740 cm^{-1} is due to the symmetric stretching mode of bridging oxygens that link the phosphate tetrahedra [17]. The base glass appears to have additional phosphate anions in the structure. The shoulder on the high frequency side of the Q^1 P-nonbridging oxygen stretching peak is likely due to nonbridging oxygens on Q^2 tetrahedra, and the peak centered near 970 cm^{-1} can be assigned to nonbridging oxygens on Q^0 tetrahedra. The Raman spectrum of this base

glass, and its interpretation, is similar to that in a recent report on comparable binary SnO-phosphate glasses [20].

As B_2O_3 is added to the base glass in both series I and II, the peak at 1050 cm^{-1} broadens and shifts to lower frequencies, to ~970 cm^{-1} for series II with ≥10 mole% B_2O_3. In addition, the peak at 740 cm^{-1} disappears from the spectra from both series, at ~13 mole% in series I and ~7 mole% in series II. These changes are consistent with the replacement of pyrophosphate units with isolated, orthophosphate units in the glass structure.

Raman peaks exclusively associated with borate vibrational modes are less easy to resolve in these spectra. Broad peaks in the 650-720 cm^{-1} range have been reported for Sn-borate [21] and Sn-borophosphate glasses [10] and assigned to metaborate units. However, there are peaks in the spectrum from the borate-free base glass in the same frequency range, making assignment of similar features to borate modes in the borophosphate spectra uncertain. A broad peak centered near 1400 cm^{-1} appears in the spectra of rapidly-quenched series II glasses with B_2O_3 contents >10 mole%. This peak has been associated with the B-O stretching modes from trigonal borons in metaborate structures [22-24].

The Raman peaks below about 500 cm^{-1} may be associated with other phosphate vibrational modes, as well as Sn(II)-O vibrational modes. Gejke et al. [10] assigned strong features near 150 and 270 cm^{-1} to Sn-O vibrations in different borate and phosphate environments, respectively.

The ^{11}B NMR spectra of the glasses from series I and II are presented in Figure 9(a) and 9(b), respectively. In series I, a symmetric peak centered near -1.7 ppm

dominates the spectra from low B_2O_3 glasses (<10 mole%), and a second peak, centered at 0.8 ppm, increases in relative intensity with increasing B_2O_3-content. A broad, asymmetric resonance, ranging from 5 to 20 ppm, is apparent in the spectra from series I glasses with ≥16% B_2O_3. Similar spectral trends are apparent for series II glasses, although the relative intensities of the peak at 1.3 ppm and the broad resonance centered near 15 ppm are both greater in series II than in series I for comparable B_2O_3-contents.

Similar ^{11}B NMR spectral changes have been reported for $xB_2O_3 \cdot (100\text{-}x)(66.7ZnO \cdot 33.3P_2O_5)$ glasses [13-14], and for other borophosphate glasses [7,25], and the peak assignments made in those studies are used here. The narrow, symmetric peak that forms on the initial addition of B_2O_3 to these glasses, centered around -1.8 ppm, is assigned to tetrahedral borons in a borophosphate structure ($B(OP)_4$). Other tetrahedral borons, with increasing numbers of boron next-nearest neighbors, $B(OP)_{4-x}(OB)_x$, account for the symmetric peaks that are evident in both sets of spectra between -1 and +2 ppm for glasses with greater B_2O_3-contents. The broad, asymmetric peak in the range of 5 to 20 ppm is assigned to trigonal borate units, BO_3.

4. DISCUSSION

Clear, colorless glasses can be prepared by modifying a $66.7SnO \cdot 33.3P_2O_5$ base glass with up to 28 mole% B_2O_3. Small additions (1-4 mole%) of B_2O_3 have significant effects on the crystallization behavior of the glass, as indicated by the elimination of the crystallization exotherm in the DTA scans of glasses from both series I and II (Figure 2). Harada et al. [26] noted a similar effect of B_2O_3 on the crystallization tendency of a Ba-

metaphosphate glass, and related it to the thermal stability of a relatively complex borophosphate glass structure, compared to a simpler, stoichiometric phosphate network.

The Raman and NMR spectra provide information about the systematic changes in glass structure when B_2O_3 is added to the Sn-pyrophosphate base glass that helps explain the compositional dependencies of the glass properties. The ^{11}B NMR spectra in Figure 9 show that B_2O_3 is initially incorporated into the glass structure as tetrahedral borophosphate units, likely with four P-tetrahedra as next-nearest neighbors, $B(OP)_4$. Additional tetrahedral sites, now with borons replacing phosphorus in the next-nearest-neighbor positions, $B(OP)_{4-x}(OB)_x$, appear in glasses with greater B_2O_3-contents. A similar conversion from tetrahedral borophosphate units to tetrahedral 'borate' units was noted by Koudelka et al [25] in their ^{11}B NMR study of Zn-Ti-borophosphate glasses. Trigonal borons can be detected in the structures of series I glasses at ~16 mole% B_2O_3 and in series II glasses at ~10 mole% B_2O_3. The Raman spectra indicate that the pyrophosphate (Q^1) species that dominate the structure of the $66.7SnO\cdot 33.3P_2O_5$ base glass are systematically replaced by isolated Q^0 units as B_2O_3 is added to the composition. A greater number of Q^0 sites are formed when an equivalent fraction of B_2O_3 is added to series II, consistent with the greater relative compositional O/P ratio.

These spectral changes, and the effects of composition on the properties of these glasses, can be explained by a simple structural model that was developed in part to explain the composition-structure relationships for Zn-borophosphate glasses [13]. Consider the following structural reactions:

$$3Sn_2P_2O_7 + B_2O_3 \rightarrow 2BPO_4 + 2Sn_3(PO_4)_2 \quad (1a)$$

$$6Q^1 + 2B[3] \rightarrow 2(B[4]_P + Q^0) + 4Q^0 \quad (1b)$$

Here, with the addition of B_2O_3, the Q^1 P-sites associated with the Sn-pyrophosphate base material are replaced by Q^0 units associated with both the $B[4]_P$ units of the 'BPO_4' product and with SnO. This reaction accounts for the general spectral trends, particularly for the series I glasses, but not necessarily for the quantitative changes in glass structure.

The complete transformation of the Q^1 P-tetrahedra to Q^0 tetrahedra, as indicated by reaction 1, should occur when the O/P ratio equals 4.0, assuming that no separate borate-rich network forms; in series I, this occurs when the B_2O_3-content is 25 mole%. For series II, where B_2O_3 replaces P_2O_5, the O/P ratio equals 4.0 when the B_2O_3 content is 8.33 mole%. Glasses with greater B_2O_3-contents must incorporate borate species in different ways than are indicated by reaction 1. The ^{11}B NMR spectra from glasses with greater B_2O_3-contents, particularly in series II, indicate that trigonal borates and tetrahedral borates with borons replacing phosphorus as next-nearest-neighbors, are present in these structures, in addition to the sites indicated in reaction (1). Trigonal borons in chains and rings are associated with metaborate crystals as well as smaller pyroborate and orthoborate units [22], and these units likely account for the high frequency (1400 cm^{-1}) band seen in the Raman spectra from the series II glasses with B_2O_3-contents $\geq$10 mole% (Figure 8(b)). This assignment is supported by the observation that glasses with relatively large B[3]-components to their ^{11}B NMR spectra have the greatest Raman intensity near 1400 cm^{-1}.

The effects of composition on the properties of the Sn-borophosphate glasses are consistent with the general structural model. The initial addition of B_2O_3 to the Sn-pyrophosphate base glass increases the glass transition temperature (Figure 3) because of the formation of tetrahedral borons which link neighboring phosphate anions with relatively strong covalent B-O-P bonds. Additions of B_2O_3 beyond ~7 mole% to series II have less effect on the glass transition temperature because of the incorporation of weaker, trigonal borons in borate-rich structural sites. The systematic decrease in aqueous corrosion rate with B_2O_3-additions (Figure 6) is also consistent with the formation of chemically stable $B[4]_P$ units that link Sn-phosphate anions. Ray [12] proposed a similar mechanism to explain the improvement in chemical durability of phosphate glasses with B_2O_3-additions. Buhrmaster et al. [7] note that small additions of B_2O_3 greatly improve the durabilities of SnO-ZnO-P_2O_5 glasses, particularly when 'BPO_4' sites form in the glass structure.

The density and refractive index (Figure 4 and Figure 5) depend principally on the SnO-concentrations, but the replacement of P_2O_5 by B_2O_3 in series II also systematically increases both properties. The incorporation of $B[4]_P$ sites decreases the molar volume of both glass series, particularly series II, compared with the Sn-pyrophosphate base glass (Figure 4). A decrease in molar volume will contribute to increases in both density and refractive index. Density and refractive index fall off with B_2O_3 additions beyond ~10 mole% for both series. This is the compositional range where the ^{11}B NMR spectra indicate that a 'borate-rich' network begins to form with tetrahedral borons not exclusively bonded to phosphorus next-nearest-neighbors and by increasing

concentrations of trigonal borons. The MV data for series I level out in this same compositional range.

The compositional dependence of the position of the UV-edge (Figure 7) for the two series is interesting. As noted by Ehrt [9], absorption at the UV-edge is due to electronic transitions associated with the Sn^{2+} ions. The systematic red-shift in the edge position when B_2O_3 replaces P_2O_5 in series II may reflect the systematic changes in the average Sn^{2+} environment as the glass converts from first a pyrophosphate network, then an orthophosphate/borophosphate network, and finally to a 'borate-rich' network. Although similar structural changes are occurring in series I, these glasses also possess systematically lower SnO-contents with increasing B_2O_3-concentrations, and this might counter the effects of changing the average Sn^{2+} chemical environment.

5. CONCLUSION

The addition of B_2O_3 to a Sn-pyrophosphate base glass increases the glass transition temperature and decreases the aqueous corrosion rate because tetrahedral borophosphate ($B[4]_P$) sites are incorporated into the glass structure. The formation of covalent B-O-P bonds produces a stronger, more chemically-resistant network. Further additions of B_2O_3 produce a more complex 'borate-rich' borophosphate network, with different tetrahedral and trigonal borate units. The relative concentrations of 'borophosphate' and 'borate' species depend on the O/P compositional ratio. This work indicates that optically transparent, chemically-durable, low-T_g compositions are possible in the SnO-B_2O_3-P_2O_5 glass-forming system.

ACKNOWLEDGEMENTS

The authors thank Manikantan Nair (Chemistry Department, Missouri S&T) for collecting the 11B NMR spectra. The financial support of the Government of the Republic of China (project No. 97-EC-17-A-08-S1-033) is gratefully acknowledged.

REFERENCES

[1] P.A. Tick, Phys. Chem. Glasses, 25 (1984) 149.

[2] C.M. Shaw and J.E. Shelby, Phys. Chem. Glasses, 29 (1988) 87.

[3] R.K. Brow, C.C. Phifer, X.J. Xu, and D.E. Day, Phys. Chem. Glasses, 33, (1992) 33.

[4] D. Holland, A.P. Howes, M.E. Smith, and A.C. Hannon, J. Phys. Condens. Matter, 14 (2002) 13609-21.

[5] T. Kikutani, US Patent 6,309,989, issued Oct. 30, 2001.

[6] T. Yamanaka, US Patent 6,306,783, issued Oct. 23, 2001.

[7] CL Buhrmaster, R. Morena, KP Reddy, and RE Youngman, US Patent 6,737,375, issued May 18, 2004.

[8] H. Takebe, W. Nonaka, T. Kubo, J. Cha, and M. Kuwabara, J. Phys. Chem. Solids, 68 (2007) 983-86.

[9] D. Ehrt, J. Non-Cryst. Solids, 354 (2008) 546-552.

[10] C. Gejke, E. Zanghellini, J. Swenson and L. Börjesson, J. Power Sources, 119-121 (2003) 576-580.

[11] T. Konishi, A. Hayashi, K. Tadanaga, T. Minami, and M. Tatsumisago, J. Non-Cryst. Solids, 354 (2008) 380-385.

[12] N.H. Ray, Inorganic Polymers, Academic Press, London, 1978, pp. 79-90.

[13] R.K. Brow, J. Non-Cryst. Solids, 194 (1996) 267-273.

[14] R.K. Brow and D. R. Tallant, J. Non-Cryst. Solids, 222 (1997) 396-406.

[15] L. Koudelka and P. Mosner, Mater. Lett., 42 (2000) 194-199.

[16] R. Morena, J. Non-Cryst. Solids, 263&264 (2000) 382-387.

[17] R.K. Brow, D.R. Tallant, S.T. Myers, and C.C. Phifer, J. Non-Cryst. Solids, 191 (1995) 45-55.

[18] J. J. Hudgens, R. K. Brow, D. R. Tallant, and S.W. Martin, J. Non. Cryst. Solids, 223[1,2] (1998) 21-31.

[19] A. Hayashi, T. Konishi, K. Tadanaga, T. Minami, and M. Tatsumisago, J. Non-Cryst. Solids, 345&346 (2004) 478-483.

[20] J. Cha, T. Kubo, H. Takebe, and M. Kuwabura, J. Cer. Soc. Japan, 116[8] (2008) 915-919.

[21] A. Hayashi, M. Nakai, M. Tatsumisago, T. Minami, Y. Himei, Y. Miura, and M. Katada, J. Non-Cryst. Solids, 306 (2002) 227-37.

[22] W.L. Konijnendijk and J. M. Stevels, J. Non-Cryst. Solids, 18 (1975) 307-331

[23] G.D. Chryssios, J.A. Kapoutsis, A.P. Patsis, E.I. Kamitsos, Spectrochim Acta, 47A[8] (1991) 1117-26

[24] RK Brow, DR Tallant and GL Turner, J. Am. Ceram. Soc., 79[9] 2410-16 (1996)

[25] L. Koudelka, P. Mosner, J. Pospisil, L. Montagne, and G. Palavit, J. Solid State Chem., 178 (2005) 1837-1843.

[26] T. Harada, H. In, H. Takebe, and K. Morinaga, J. Amer. Ceram. Soc., 87[3] (2004) 408-411.

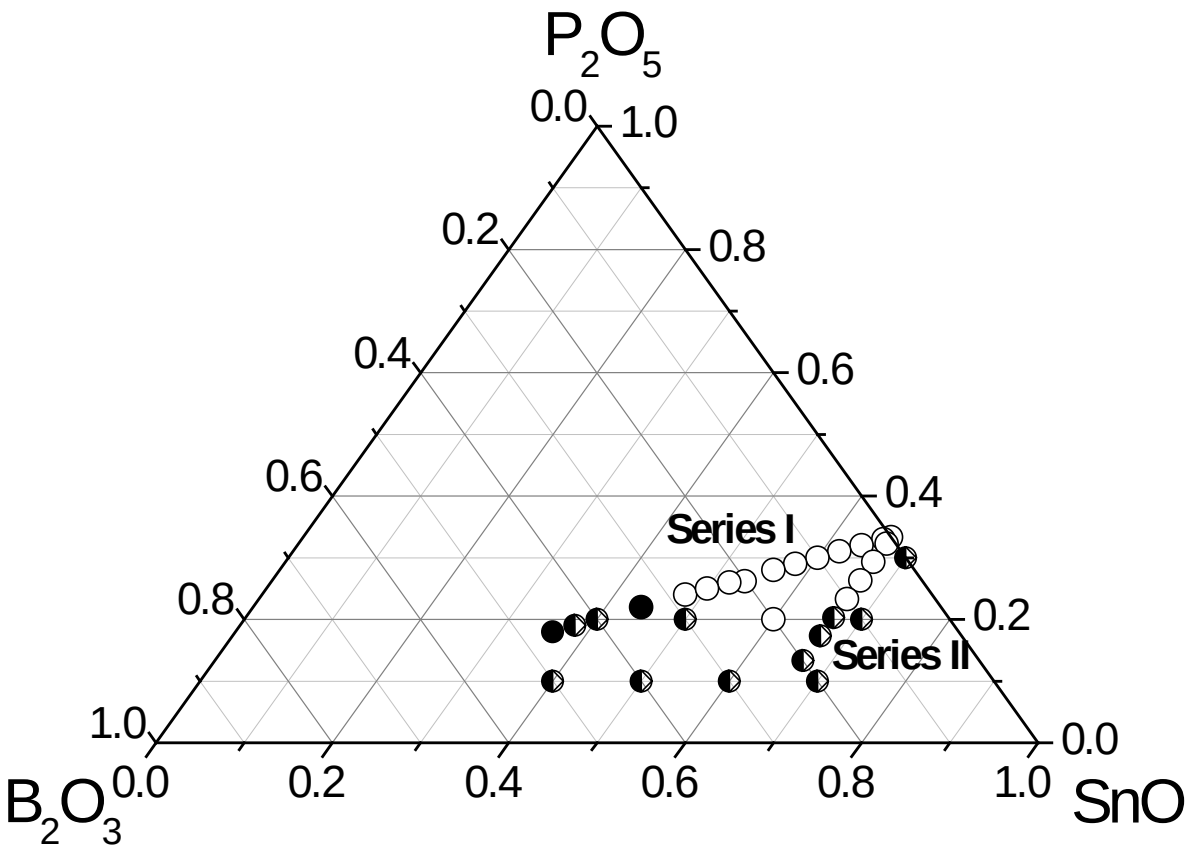

Figure 1. Molar compositions of samples prepared in this study. Open circles represent compositions that form homogeneous glasses at 900°C; half-closed circles are those compositions that were partially crystallized upon quenching.

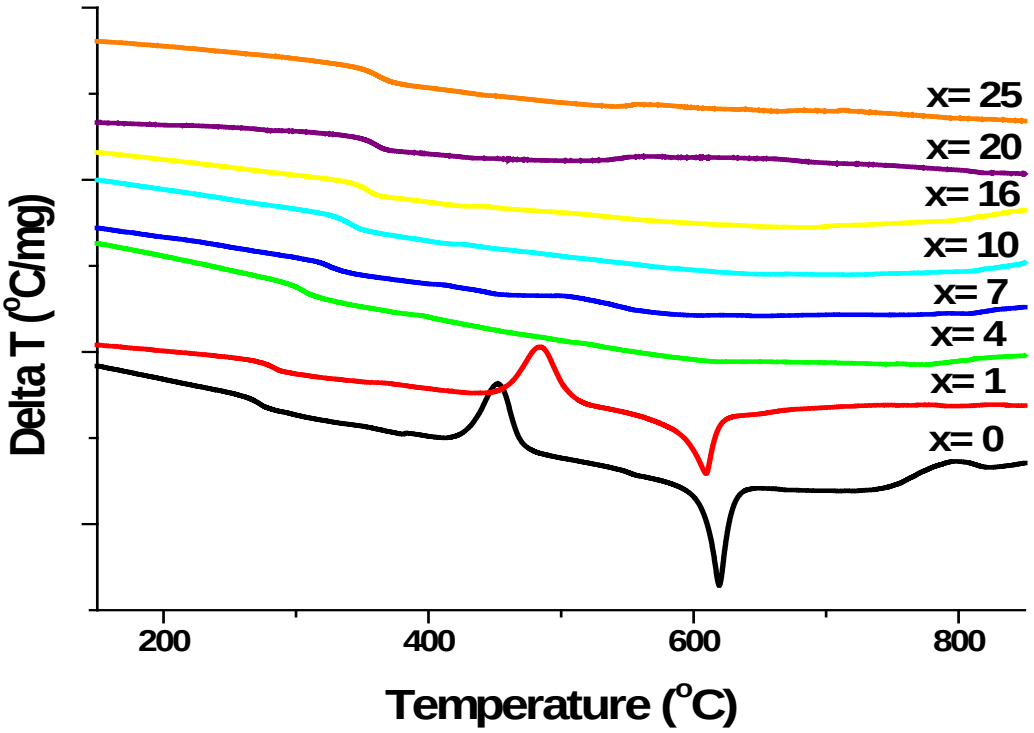

(a)

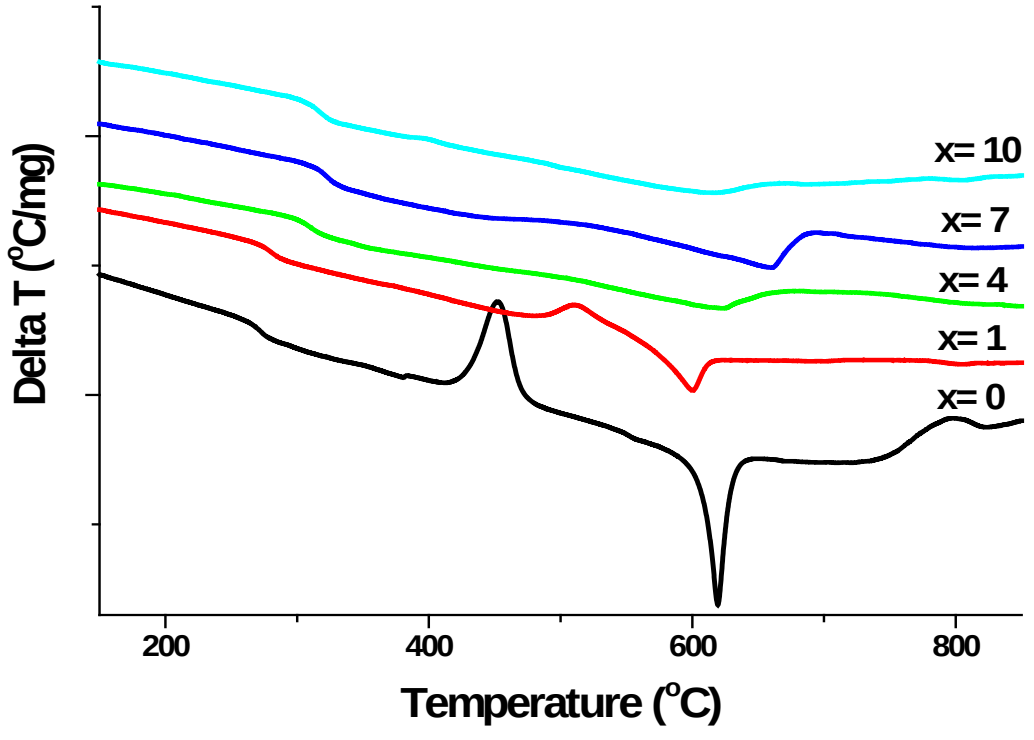

(b)

Figure 2. DTA curves collected from the Sn-borophosphate glasses in (a) series I and (b) series II.

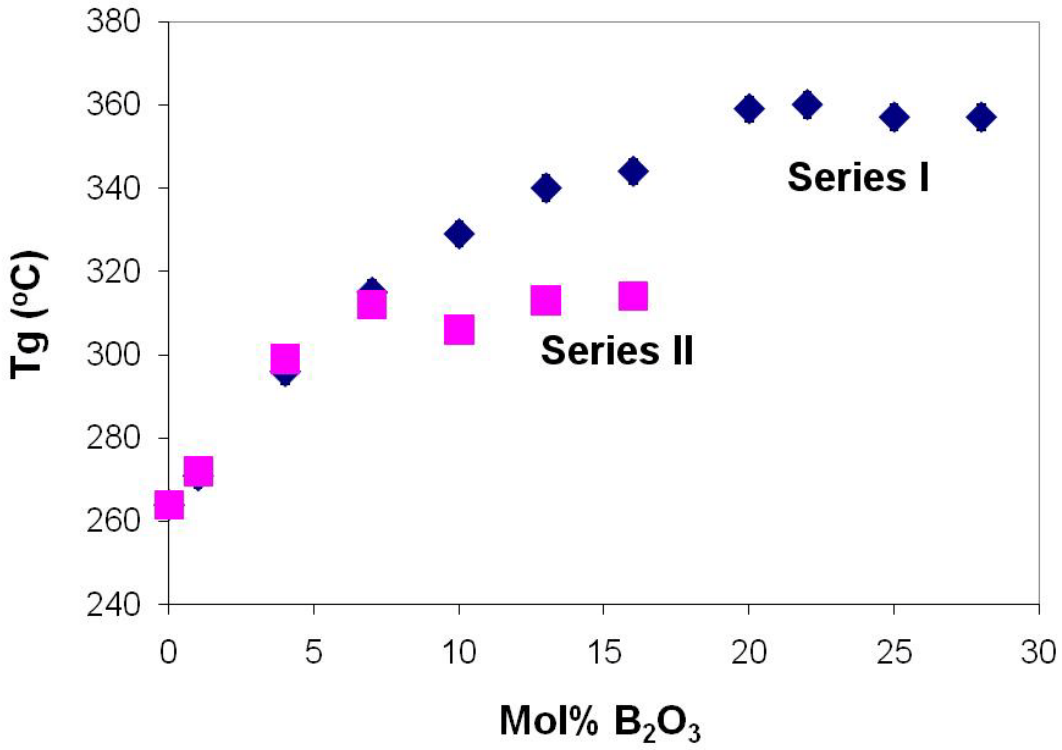

Figure 3. The effect of B_2O_3 content on the glass transition temperature of Sn-borophosphate glasses.

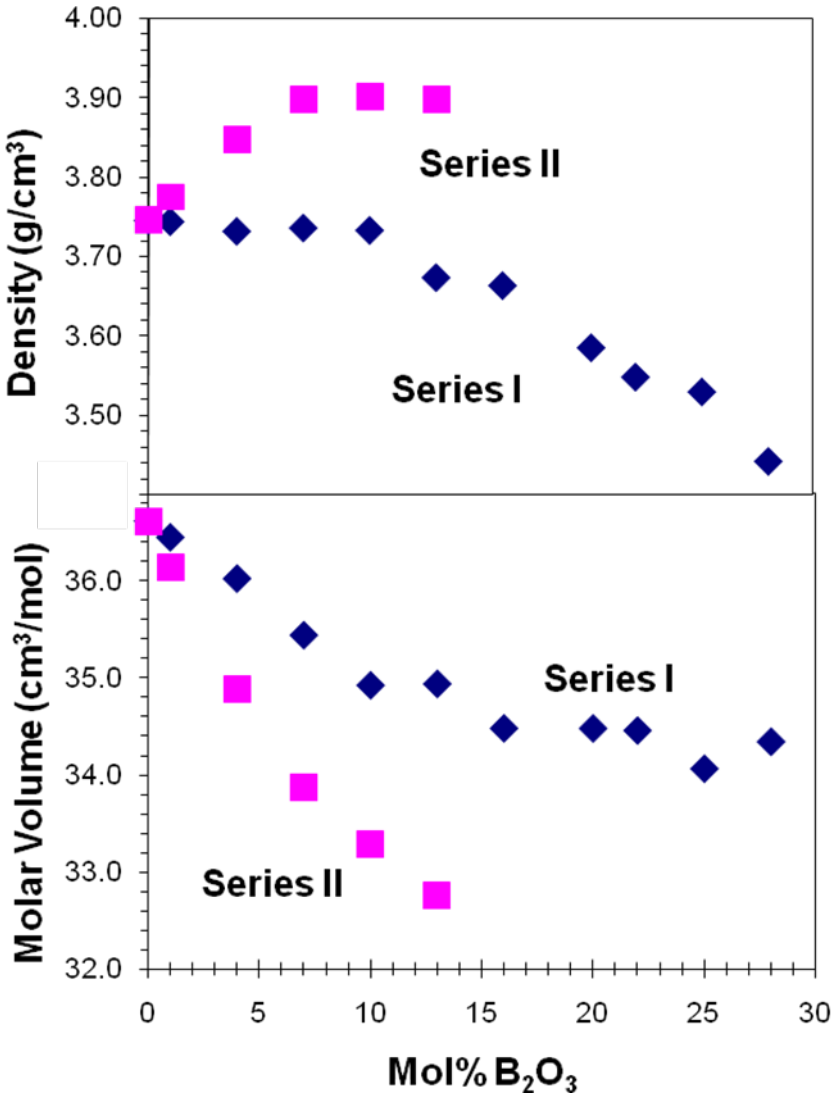

Figure 4. The effect of B_2O_3 content on the density and molar volume of Sn-borophosphate glasses.

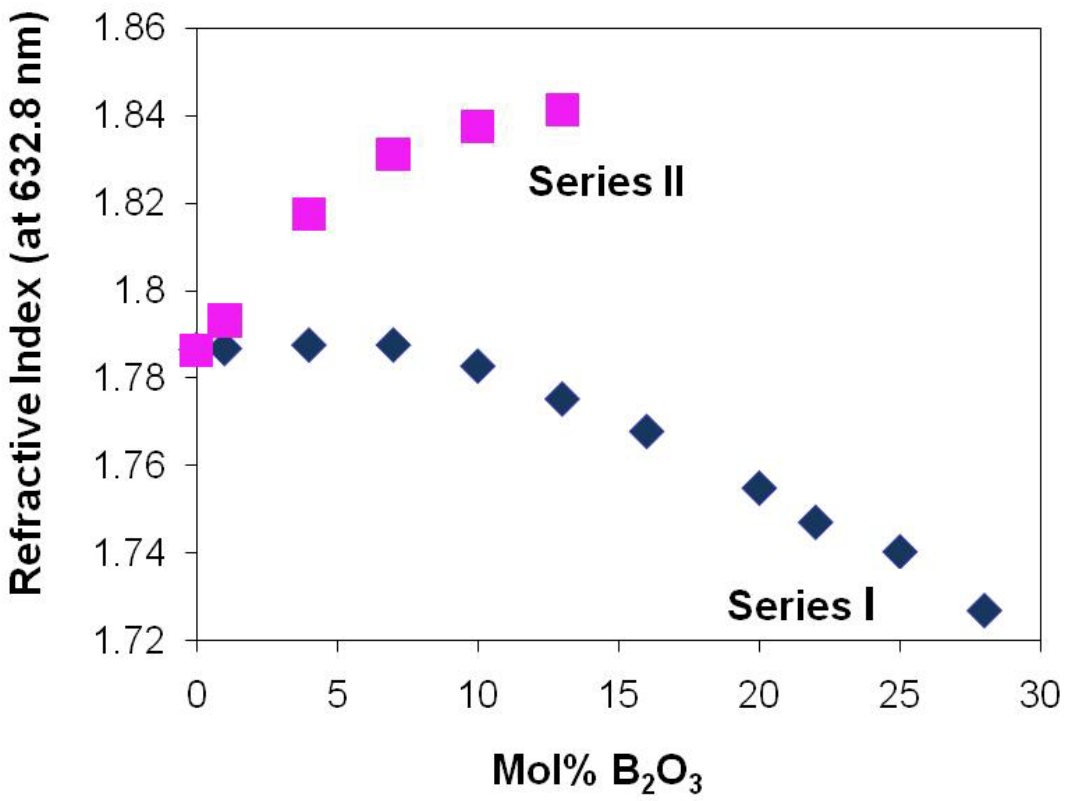

Figure 5. The effect of B_2O_3 content on the refractive index of Sn-borophosphate glasses.

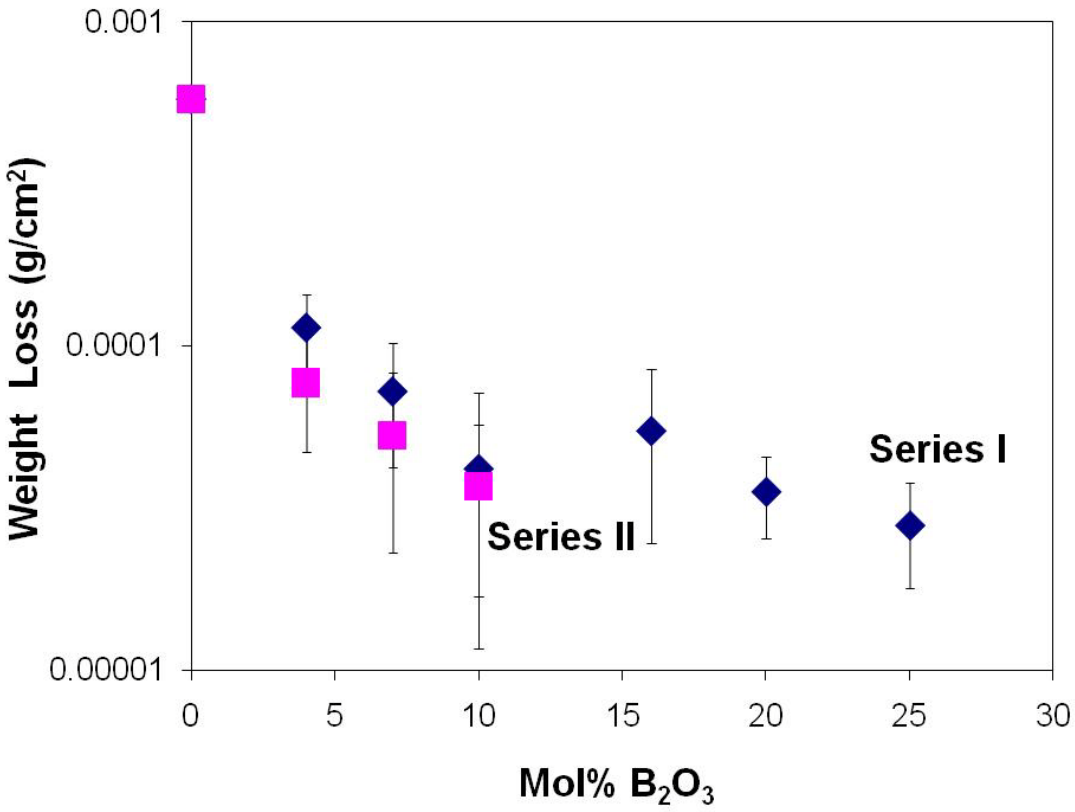

Figure 6. The effect of B_2O_3 content on the weight loss of Sn-borophosphate glasses after 24 hours in 40°C water.

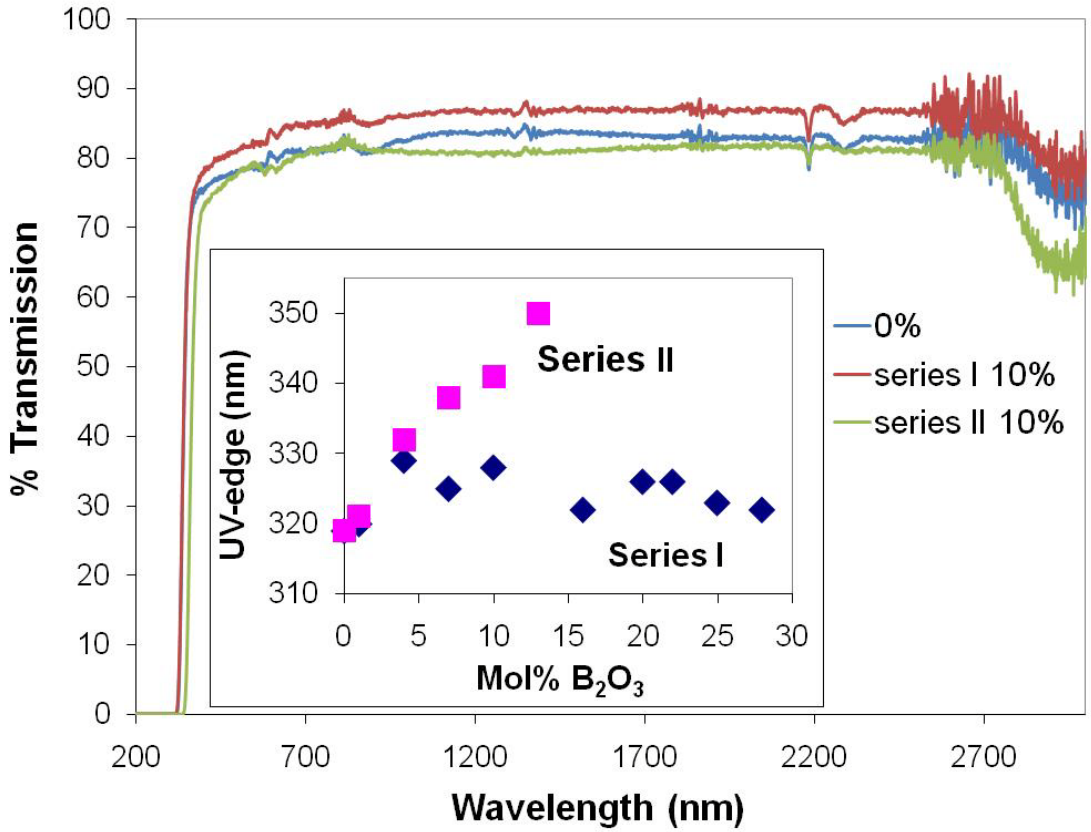

Figure 7. Optical transmission spectra of representative Sn-borophosphate glasses; the inset shows the effect of B_2O_3-content on the UV-edge for both glass series.

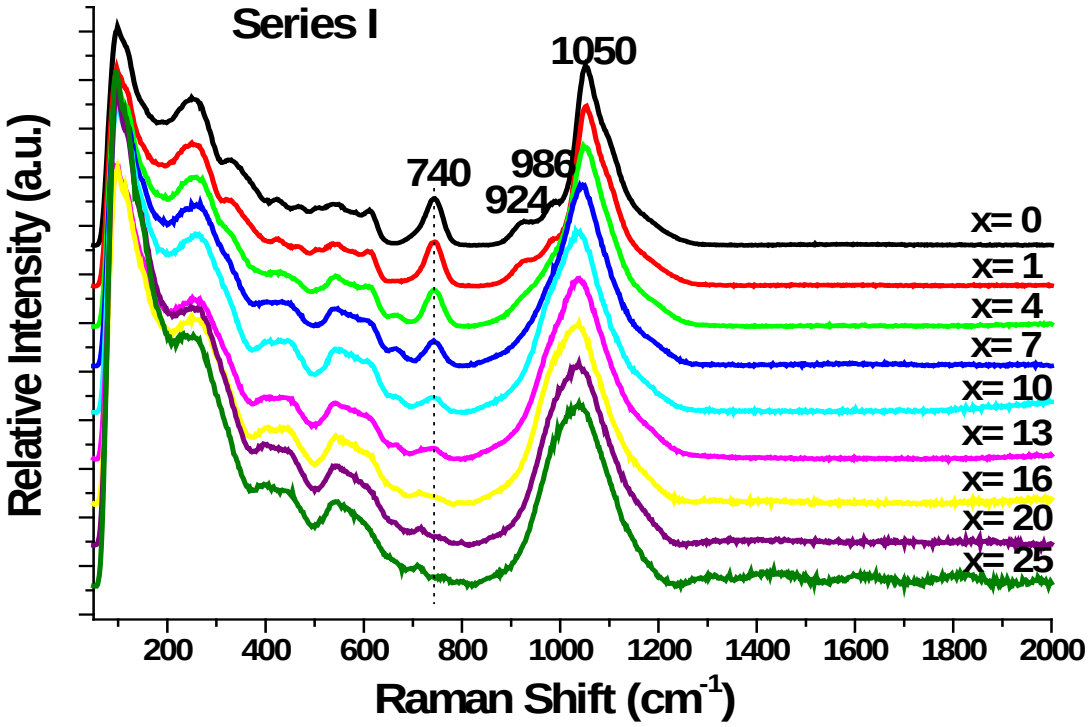

(a)

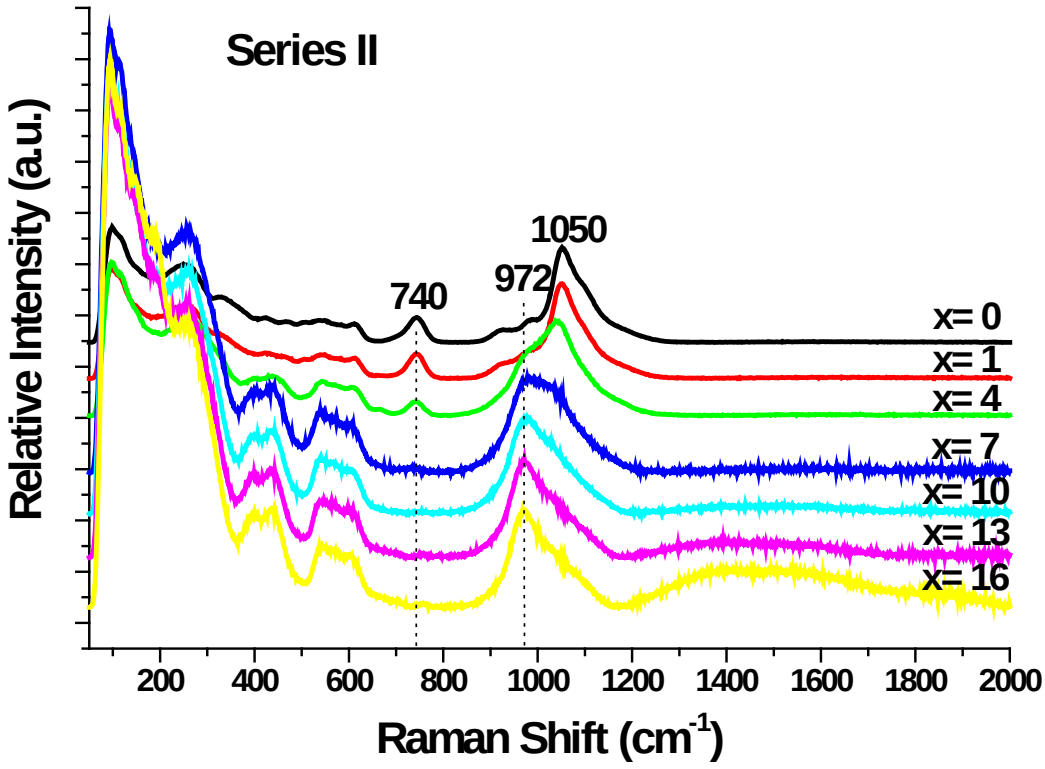

(b)

Figure 8. Raman spectra of Sn-borophosphate glasses, (a) series I, and (b) series II.

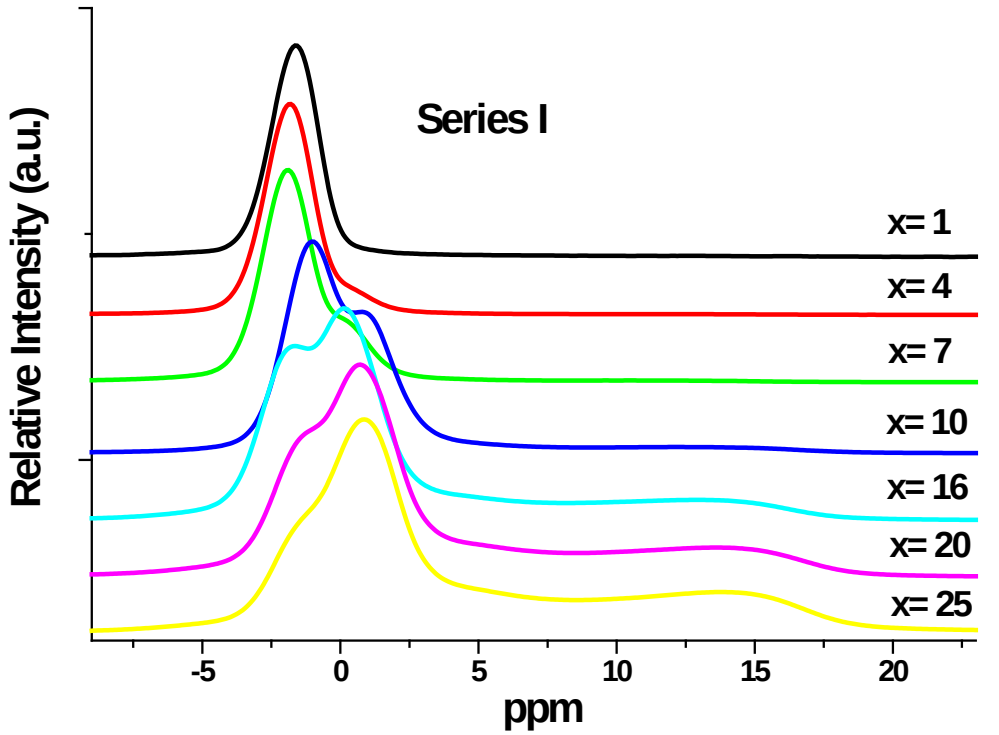

(a)

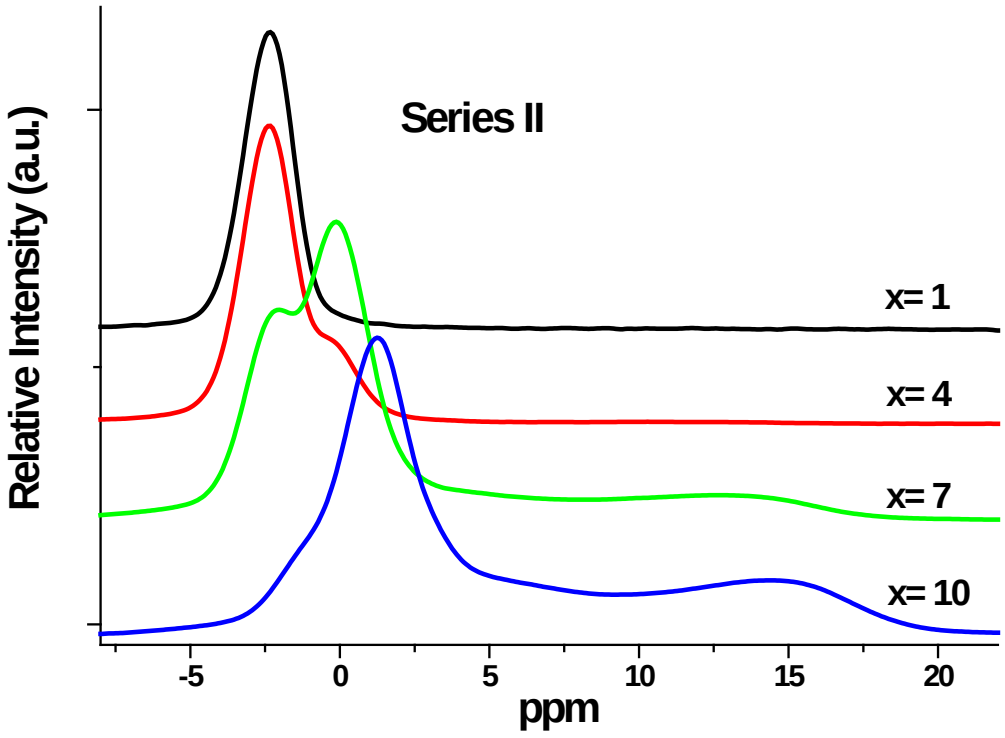

(b)

Figure 9. ^{11}B NMR spectra of Sn-borophosphate glasses, (a) series I, and (b) series II.

III. PROPERTIES AND STRUCTURE OF TIN PHOSPHATE GLASSES MODIFIED WITH Ga_2O_3 and Sb_2O_3

J.W. Lim [a], S.W. Yung [b] and R.K. Brow [a]

[a] *Missouri University of Science & Technology,* Department of Materials Science & Engineering, Rolla, MO 65409 USA

[b] *National United University*, Department of Materials Science & Engineering, Miao-Li 36003, Taiwan, ROC

ABSTRACT

The properties and structure of 66.7SnO*33.3P_2O_5(mol%) glasses modified with Ga_2O_3 and Sb_2O_3 are reported. The glasses were melted in a vitreous carbon crucible under argon at 1000°C to avoid oxidation of Sn(II). Differential thermal analysis (DTA) was used to determine glass transition temperature (T_g), which increased from 264°C to 339°C with the addition of 13 mole% Ga_2O_3 and to 311°C with the addition of 7 mole% Sb_2O_3. The dissolution rates in deionized water decrease by an order of magnitude with the addition of both oxides to the tin phosphate base glass. A prism coupling technique was used to measure the refractive index at three different wavelengths. When Ga_2O_3 is added to the base glass, the refractive index (at 632.8 nm) decreases slightly, from 1.7865 to 1.7709 (13 mol%); when Ga_2O_3 replaces P_2O_5 in the base glass, the refractive index increases to 1.829 (7 mol%). The addition of Sb_2O_3 to the base glass increases refractive index to 1.816 (7 mol%). From the Raman spectra, the addition of Ga_2O_3 and Sb_2O_3 leads to the formation of isolated phosphate tetrahedra (Q^0 units) that link with Ga- and Sb-polyhedra to form the glass network.

1. INTRODUCTION

Glasses from the tin(II) phosphate system have high refractive indices and low glass transition temperatures, making them good candidate materials for producing precision molded optical components. Previous studies report that the composition $67SnO\text{-}33P_2O_5$ (mol%) has a refractive index (n_d) of 1.794 and a glass transition temperature of 268°C [1]. For the $60SnO\text{-}40P_2O_5$ binary composition, the glass transition temperature is reported to be 300°C with the refractive index (n_d) and Abbe number (ν_d) are 1.762 and 26.7, respectively [2]. However, phosphate glasses often have poor chemical durability, limiting their application. Adding other oxides to tin phosphate base glasses will modify the glass network and alter glass properties, including chemical durability. Recently, the properties of tin pyrophosphate ($66.7SnO\text{-}33.3P_2O_5$ (mol%)) glasses modified with B_2O_3 were reported [3]. Chemically durable tin borophosphate (SBP) compositions with high refractive indices (>1.78) and low glass transition temperatures (<300ºC) were described.

Other oxides are candidates for modifying glass compositions designed for optical applications. For example, gallium-based glasses have been developed for IR transmission and with large non-linear optical susceptibilities [4]. Binary gallium phosphate glasses with up to 40 mol% Ga_2O_3 have been studied by Raman and IR spectroscopy [5], which reveal networks of ortho-, pyro-, and polyphosphate anions interconnected by tetrahedral GaO_4 units. Glasses containing Sb_2O_3 also have low melting temperatures. Koudelka *et al.* [6] reported that the incorporation of Sb_2O_3 into a zinc borophosphate network of $50ZnO\text{-}10B_2O_3\text{-}40P_2O_5$ glasses modified its structure and

decreased the T_g. However, the optical properties of tin phosphate glasses containing Ga_2O_3 and Sb_2O_3 have not been reported.

In this paper, the effects of the addition of Ga_2O_3 and Sb_2O_3 on the properties of tin phosphate glasses are reported. Information about the compositional dependencies of the phosphate anions that constitute the glass structure is obtained by Raman spectroscopy.

2. EXPERIMENTAL METHOD

Two series of tin phosphate glasses modified by Ga_2O_3 were prepared from reagent grade SnO (Alfa Aesar, 99.9%), $Sn_2P_2O_7$ (Alfa Aesar), and Ga_2O_3 (Johnson Matthey Chemicals, 99.99%). In series I, Ga_2O_3 was added to a $66.7SnO{\cdot}33.3P_2O_5$ base glass according to $xGa_2O_3{\cdot}(100\text{-}x)(66.7SnO{\cdot}33.3P_2O_5)$, and in series II, Ga_2O_3 replaced P_2O_5 in the base glass, according to $xGa_2O_3 \cdot 66.7SnO{\cdot}(33.3\text{-}x)P_2O_5$. Batches that produced 10g of glass were thoroughly mixed and then melted in a vitreous carbon crucible for 30 minutes at 1000^{o}C under flowing argon to prevent to oxidation of Sn(II). Two similar compositional series were prepared using crystalline Sb_2O_3 (Baker & Adamson), instead of Ga_2O_3, with crystalline $Sn_2P_2O_7$. These tin antimony phosphate glasses were prepared under similar conditions as those used for the tin gallium phosphate glasses.

Differential thermal analyzer (Perkin Elmer DTA 7) was used to determine T_g. About 40mg of glass (size 425~500 μm) was placed in an alumina crucible and heated at 10°C/min under nitrogen. Glass density was measured by the Archimedes method using distilled water. Aqueous corrosion rates were determined from samples approximately

10mm x 5.5mm x 1mm, polished to 1 μm a diamond suspension. The samples were suspended in 100 ml of distilled water (pH~6) in polypropylene containers held at 40°C. Samples were removed from the water at periodic intervals, dried in air for 20 minutes, and re-weighed to record weight losses. Corrosion rates reported here were determined after 24 hours of exposure.

The refractive indices of the glasses were measure by a prism coupling method (Metricon 2010) at wavelengths of 405, 632.8, and 785 nm. An Abbe number, $\nu_D=(n_D-1)/(n_F-n_C)$, was determined by calculating refractive indices at 656.3 nm (n_C), 589.3 nm (n_D) and 486.1 nm (n_F) after fitting the three measured refractive indices using the Cauchy dispersion equation:

$$n(\lambda) = a + b*\lambda^{-2} + c*\lambda^{-4} \text{ (where } \lambda \text{ is wavelength)}$$

Transmission spectra were collected from bulk samples polished to 1μm by a Cary 5 UV-Vis-NIR spectrophotometer. The UV edge was defined by the wavelength at which the samples had an absorbance of 4 cm^{-1}. Raman spectra were measured from bulk glass samples with a Jobin-Yvon micro-Raman spectrometer (LabRAM ARAMIS) with a 632.8 nm He-Ne laser.

3. RESULTS

For the Ga_2O_3 modified Sn-phosphate system ($SnO-Ga_2O_3-P_2O_5$), clear, colorless glasses were obtained with up to 13 mol% Ga_2O_3 in series I. In series II, clear and colorless glass could be cast from melts with up to 7 mol% Ga_2O_3. Higher concentration

of Ga_2O_3 made the glass crystallized or unmelted powder was found in glass form. Clear and colorless SnO-Sb_2O_3-P_2O_5 (SSbP) glasses could be prepared in series I with up to 7 mole% Sb_2O_3. These samples formed glass without any surface crystallization. Adding 1 mole % Sb_2O_3 to series II produced a partially crystallized sample when the conventional melt process conditions were used. Greater concentrations of Sb_2O_3 produced yellow glasses. For each glass series, weight losses of about 2% occurred during melting and the nominal (batched) compositions will be used to describe trends in properties and structures.

Table 1 lists the properties for the Sn(II)- Ga(III)-phosphate glasses from series I and series II, and Table 2 summarizes the properties for the Sn(II)-Sb(III)-phosphate glasses from series I.

The addition of both Ga_2O_3 and Sb_2O_3 to the Sn-pyrophosphate base glass increases the glass transition temperature (T_g). The densities and molar volumes of both modified glass series are shown in Figure 1. The densities of both glass systems increase with the addition of these modifying oxides (Figure 1(a)) whereas the molar volumes, calculated from these densities and the respective molecular weights of the nominal compositions, exhibit more complicated behavior. Molar volume increases with the addition of both Ga_2O_3 and Sb_2O_3 in series I, but decreases when Ga_2O_3 replaces P_2O_5 in series II (Figure 1(b)).

Figure 2 shows the compositional dependencies of the refractive index for the modified tin phosphate glasses. Ga_2O_3 additions decrease the refractive index (at 632.8 nm) of glasses in series I, but increase the refractive index of glasses in series II. The refractive index increases with increasing Sb_2O_3 in series I.

Figure 3 shows the weight loss of the modified tin phosphate glasses after immersion in water at 40°C for 24 hrs. The weight loss decreases with the addition of both modifying oxides. A similar improvement in chemical durability was noted with the addition of B_2O_3 to the SnO-pyrophosphate base glass [3].

Figure 4 shows the optical transmission curves, from the UV through the near infrared, for several of the modified glasses. The inset to Figure 4 shows the compositional dependence of the UV edge. For each glass series, the wavelength of the edge increases systematically with the addition of the modifying oxides.

The optical dispersion of the modified tin phosphate glasses is characterized by the Abbe number, ν_D (Table 1 and Table 2). The Abbe number decreases with the addition of both Ga_2O_3 (both series) and Sb_2O_3. These trends are consistent with the red-shifts in the UV-edge with the addition of both Ga_2O_3 and Sb_2O_3, which measure refractive index of short wavelengths more than at long wavelength.

The Raman spectra from the SGaP glasses from series I and II are shown in Figure 5(a) and Figure 5(b), respectively. Figure 6 shows Raman spectra from the SnO-Sb_2O_3-P_2O_5 glasses. In Figure 5 and Figure 6, peaks in the range of 700 to 1100 cm^{-1} can be assigned to vibrational modes associated with the phosphate network and are consistent with a glass structure dominated by pyrophosphate units [7-8]. The intense band near 1050 cm^{-1} results from the symmetric P-O stretch of nonbridging oxygens on these Q^1 tetrahedra associated with pyrophosphate anions (or chain-ending units), and the sharp band at 740 cm^{-1} is due to the symmetric stretching mode of bridging oxygens that link the Q^1 phosphate tetrahedra [7].

In Figure 5, the shoulder near 1150 cm^{-1}, on the high frequency side of the Q^1 P-nonbridging oxygen stretching peak, is likely due to the asymmetric stretching modes of nonbridging oxygens on Q^1 tetrahedra, and the peak centered near 970 cm^{-1} can be assigned to stretching modes associated with nonbridging oxygens on Q^0 tetrahedra [9]. As Ga_2O_3 is added to the base glass in both series I and II, the peak at 1050 cm^{-1} broadens and shifts to lower frequencies, approaching ~970 cm^{-1}, in both series I and series II. In addition, the relative intensity of the shoulder at 1150 cm^{-1} increases with increasing Ga_2O_3. These changes are consistent with the replacement of pyrophosphate units with isolated, tetrahedral units (Q^0) in the glass structure. The band at 550~670 cm^{-1} can be assigned to the stretching vibrational modes of GaO_4 tetrahedra [5,10]. The Raman bands at 370~500 cm^{-1} may be assigned to deformation modes associated with symmetric the Ga-O-P bonds between gallate and phosphate units [5].

In Figure 6, the peak centered near 990 cm^{-1} can be assigned to stretching modes of nonbridging oxygens on Q^0 tetrahedra. As Sb_2O_3 is added to the base glass in series I, the peak at 1050 cm^{-1} broadens and shifts to lower frequencies, to ~990 cm^{-1} with > 4 mole% Sb_2O_3. In addition, the peak at 740 cm^{-1} disappears from the spectrum of glass with 7 mole% Sb_2O_3. These changes are consistent with the replacement of pyrophosphate units with isolated orthophosphate units in the glass structure. Broad peaks in the 350-680 cm^{-1} range have been reported for Sb–O vibrational modes [6] and the intensities of bands in this region increased with increasing Sb_2O_3 content. These bands have been associated with isolated SbO_3 units and with clusters of Sb-O-Sb bonds [6].

4. DISCUSSION

Clear and colorless glasses can be prepared by modifying a $66.7SnO \cdot 33.3P_2O_5$ base glass with up to 13 mole% Ga_2O_3 (series I) and by replacing P_2O_5 with up to 7 mol% Ga_2O_3 (series II). Clear and colorless glasses can be also prepared by adding up to 7 mol% Sb_2O_3 to the tin phosphate base glass. The Raman spectra provide information about the systematic changes in glass structure when these modifying oxides are added to the Sn-pyrophosphate base glass. The Raman spectra indicate that the pyrophosphate (Q^1) anions that dominate the structure of the $66.7SnO \cdot 33.3P_2O_5$ base glass are systematically replaced by isolated Q^0 units as Ga_2O_3 and Sb_2O_3 are added to the composition.

The effects of composition on the properties of the modified Sn-phosphate glasses are consistent with the general structural model. The glass transition temperature of the modified Sn-pyrophosphate glass increases because of the formation of tetrahedral gallium that links neighboring phosphate anions to create the relatively strong covalent Ga-O-P bonds [8]. The Raman spectra indicate that the addition of Ga_2O_3 and Sb_2O_3 break P-O-P bonds to form P-O-Ga (Sb) linkages.

The density and refractive index depend on the SnO-concentrations, but the replacement of P_2O_5 by Ga_2O_3 in series II also systematically increases both properties. Decreases in the molar volume with Ga_2O_3 additions in series II will contribute to increases in both density and refractive index. However, the molar volume increases with the addition of both Ga_2O_3 and Sb_2O_3 in series I and appears to expand the glass network. This behavior may be related to the number of oxygen ions in a mole of glass. The atomic fraction of oxygen increases with the addition of Ga_2O_3 and Sb_2O_3 in series I,

but decreases in series II. Since O^{2-} is the largest ion in these glasses, it will have the greatest effect on molar volume.

Phosphate glasses are known, in general, to have poor chemical durability because most metal-oxygen-phosphorus bonds that link the phosphate anions that constitute the glass structure are readily hydrated, allowing the anions to dissolve into aqueous solutions [11]. However, these P-O-Ga (Sb) bonds improve the durability of the glass samples as shown in Figure 3 because Ga_2O_3 and Sb_2O_3 form strong covalent bonds with the phosphate tetrahedra [12].

5. SUMMARY

The glass forming region of $66.7SnO*33.3P_2O_5$ glass modified with Ga_2O_3 and Sb_2O_3 is determined and their structure and properties are reported. The addition of Ga_2O_3 to a Sn-pyrophosphate base glass increases the glass transition temperature and improves the durability in water because tetrahedral phosphate sites are linked with modified oxides to form covalent Ga-O-P bonds in the glass structure, as shown in the Raman spectra collected from the glasses. The incorporation of Sb_2O_3 into the $66.7SnO*33.3P_2O_5$ glass modified their structures and properties in a similar way. The increase in the glass transition temperature and chemical durability with the addition of Sb_2O_3 is due to the creation of isolated SbO_3 units that are linked to the phosphate anions through Sb-O-P bonds. The densities and refractive indices of the glasses with different modifier oxides are determined and the results are related to changes in the molar volume of the glasses.

ACKNOWLEDGEMENTS

The authors thank Mariano Velez (Mo Sci) and Curtis Planje (Brewer Science) for helping with the refractive index measurements. The financial support of the Government of the Republic of China (project No. 97-EC-17-A-08-S1-033) is gratefully acknowledged.

REFERENCES

[1] H. Takebe, W. Nonaka, T. Kubo, J. Cha, and M. Kuwabara, J. Phys. Chem. Solids, 68 (2007) 983-86.

[2] D. Ehrt, J. Non-Cryst. Solids, 354 (2008) 546-552.

[3] J. W. Lim, M. L. Schmitt, S. W. Yung, and R. K. Brow, J. Non-Cryst. Solids, 356 (2010) 1379-1384.

[4] W.H. Dumbough, J.C. Lapp, J. Am. Ceram. Soc. 75 (1992) 2315.

[5] D. Ilieva, B. Jivov, G. Bogachev, C. Petkov, I. Penkov, and Y. Dimitriev, J. Non-Cryst. Solids, 283 (2001) 195-202.

[6] L. Koudelka, J. Šučík, P. Mošner, L. Montagne, and L. Delevoye, J. Non-Cryst. Solids, 353 (2007) 1828-1833.

[7] R.K. Brow, D.R. Tallant, S.T. Myers, and C.C. Phifer, J. Non-Cryst. Solids, 191(1995) 45-55.

[8] J. J. Hudgens, R. K. Brow, D. R. Tallant, and S.W. Martin, J. Non- Cryst. Solids, 223 [1, 2] (1998) 21-31.

[9] J. Cha, T. Kubo, H. Takebe, and M. Kuwabara, J. Ceram. Soc. Japan, 116 [8] (2008) 915-919.

[10] A. Belkébir, J. Rocha, A.P. Esculcas, P. Berthet, S. Poisson, B. Gilbert, Z. Gabelica, G. Llabres, F. Wijzen, and A. Rulmont, Spectrochimica Acta Part A, 56 (2000) 423~434.

[11] X. Yu, D. E. Day, G. J. Long, and R.K. Brow, J. Non-Cryst. Solids, 215 (1997) 21.

[12] B. Zhang, Q. Chen, L. Song, H. Li, F. Hou, and J. Zhang, J. Non-Cryst. Solids, 354 (2008) 1948-1954.

Table 1: Selected properties of the SnO-Ga_2O_3-P_2O_5 glasses.

Series I	Density (± 0.002)	Refrac. Index (± 0.0003)	Glass Trans. (± 5°C)	UV-edge (± 1)	Abbe #
Mole%	g/cm^3	(632.8 nm)	T_g (°C)	nm	ν_D
0.0	3.745	1.7865	264	319	23.38
1.0	3.802	1.7858	269	322	22.41
4.0	3.827	1.7824	285	324	22.84
7.0	3.858	1.7781	303	327	22.95
10.0	3.874	1.7733	322	334	22.87
13.0	3.879	1.7709	339	342	22.83
Series II					
1.0	3.844	1.7932	269	324	22.02
4.0	3.948	1.8110	289	333	21.17
7.0	4.044	1.8292	311	354	20.21

Table 2: Selected properties of the SnO-Sb_2O_3-P_2O_5 glasses.

Series I	Density (± 0.002)	Refrac. Index (± 0.0003)	Glass Trans. (± 5°C)	UV-edge (± 1)	Abbe #
Mole%	g/cm^3	(632.8 nm)	T_g (°C)	nm	ν_D
0.0	3.745	1.7865	264	319	23.38
1.0	3.784	1.7943	290	324	23.25
4.0	3.868	1.8023	300	332	23.21
7.0	3.920	1.8155	311	337	22.23

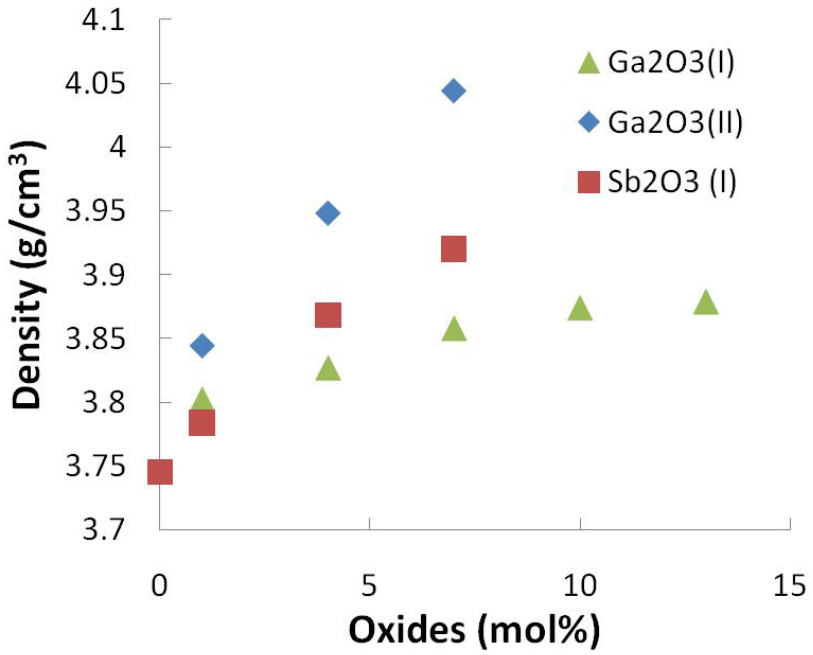

(a)

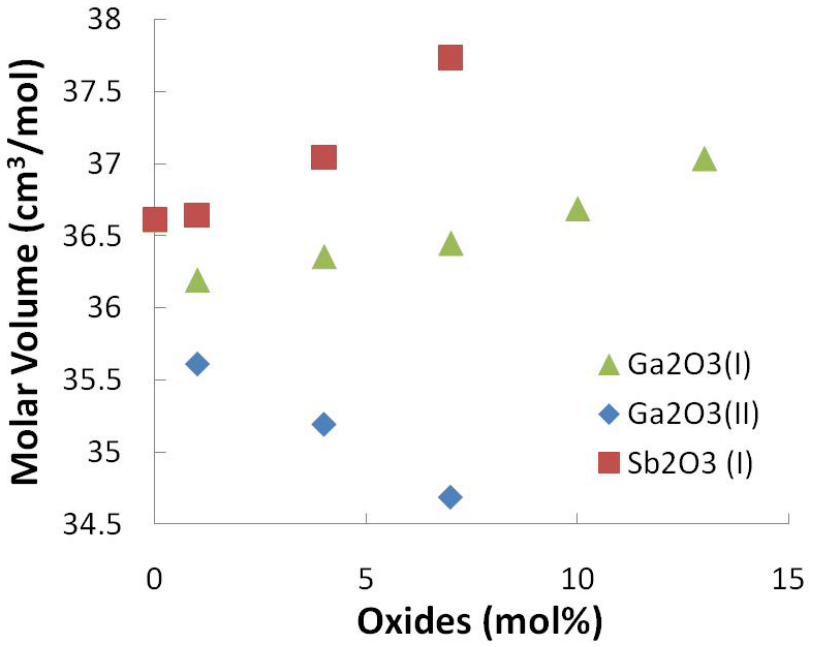

(b)

Figure 1. Density (a) and molar volume (b) of SnO-Ga_2O_3-P_2O_5 series I and series II and SnO-Sb_2O_3-P_2O_5 series I glasses.

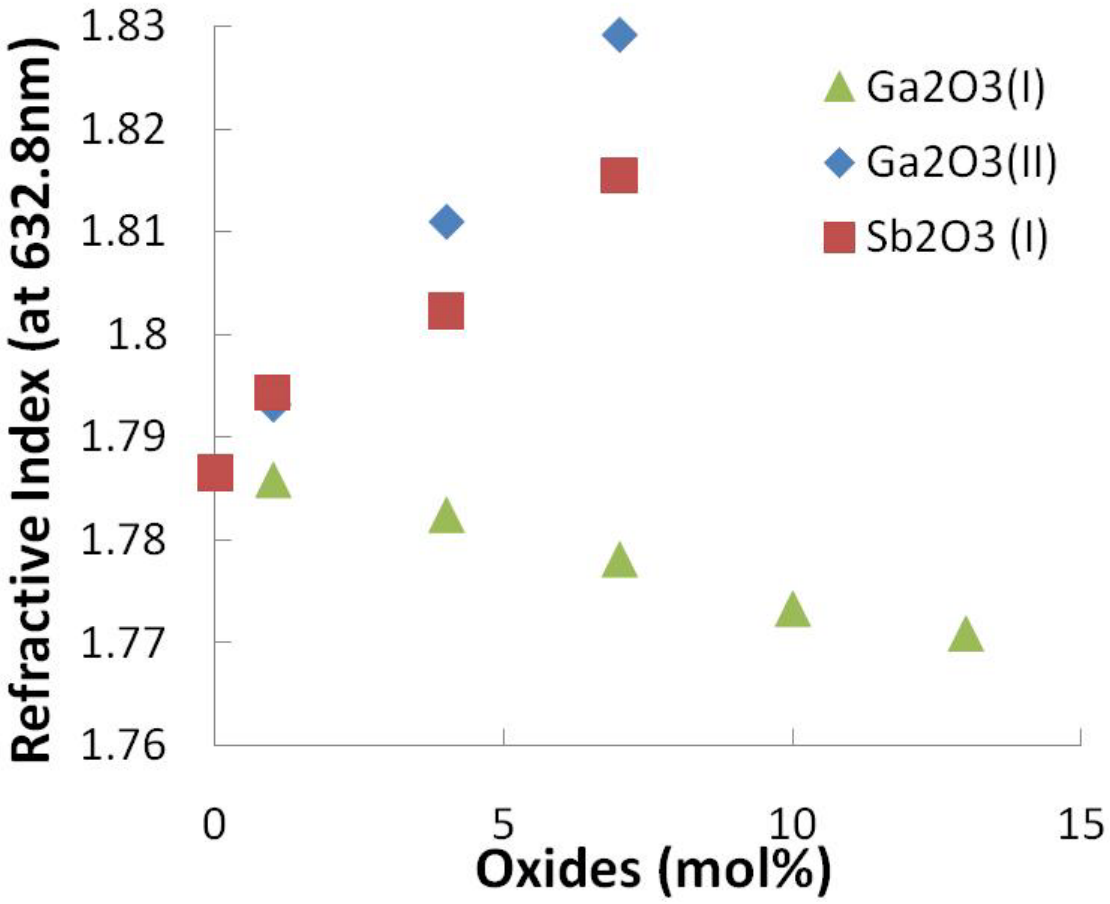

Figure 2. The refractive index of glasses from SnO-Ga_2O_3-P_2O_5 series I and series II and SnO-Sb_2O_3-P_2O_5 series I.

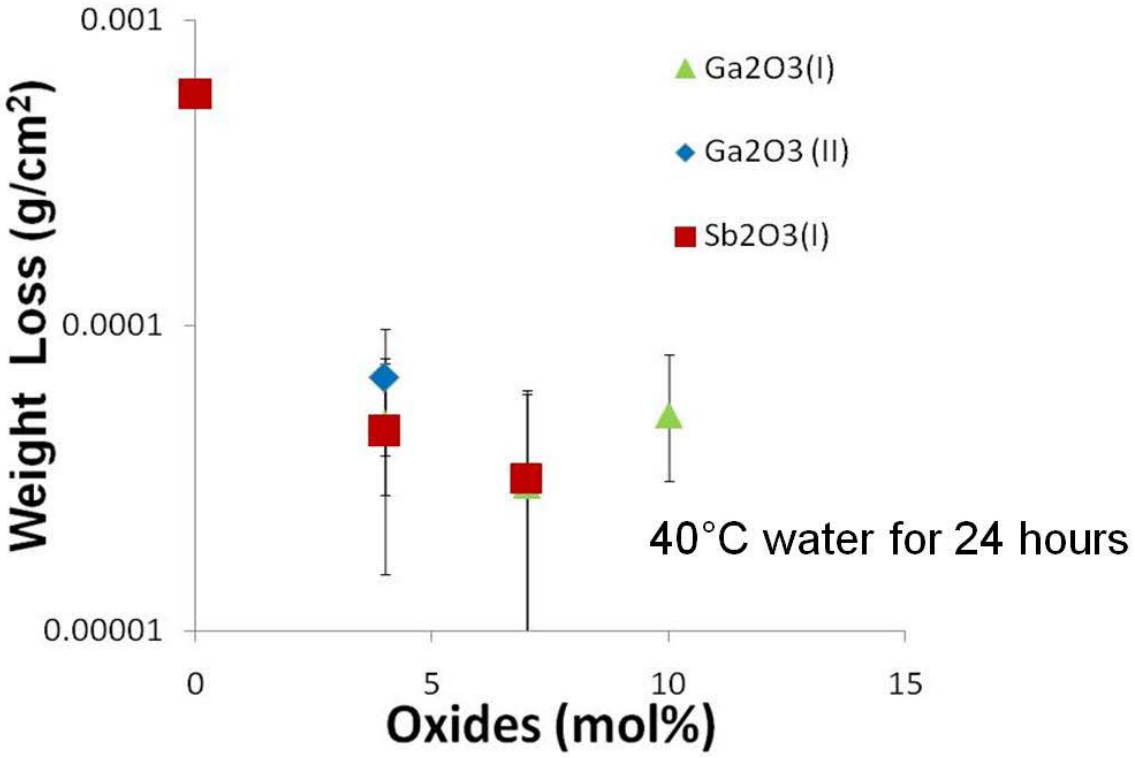

Figure 3. The effect of modified oxides content on the weight loss of tin pyrophosphate glasses in 40ºC water after 24 hours.

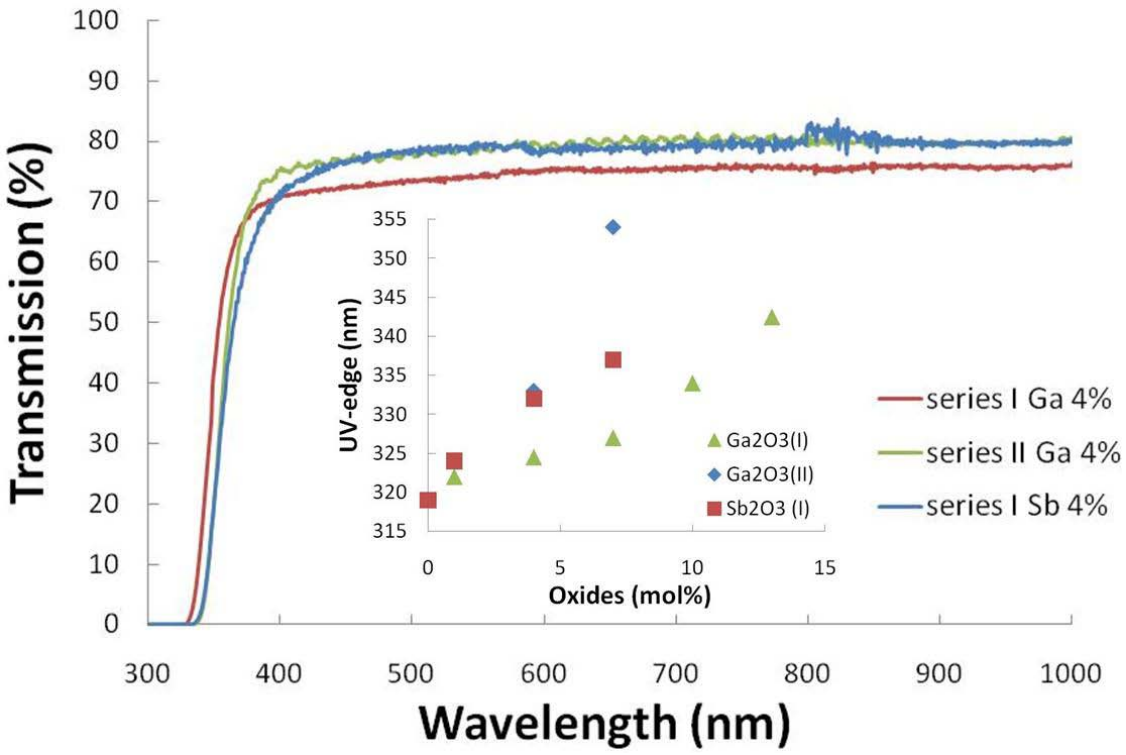

Figure 4. Transmittance spectra of modified tin phosphate glasses. Inset figure shows the absorption UV edge of modified glass samples.

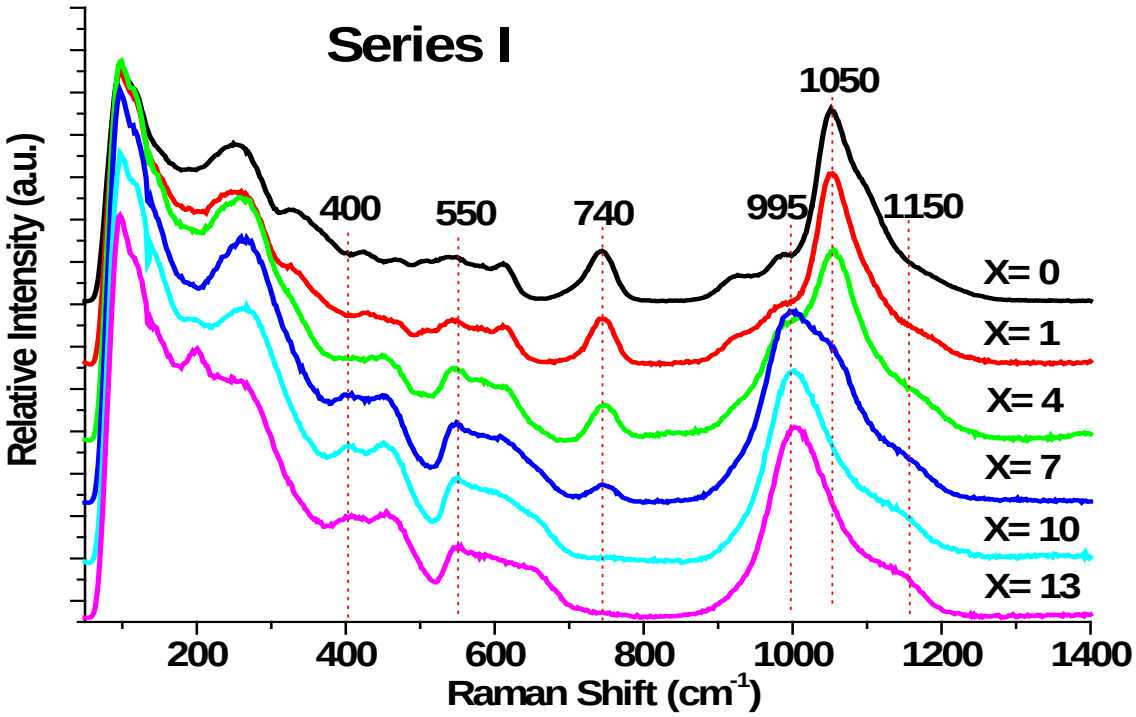

(a)

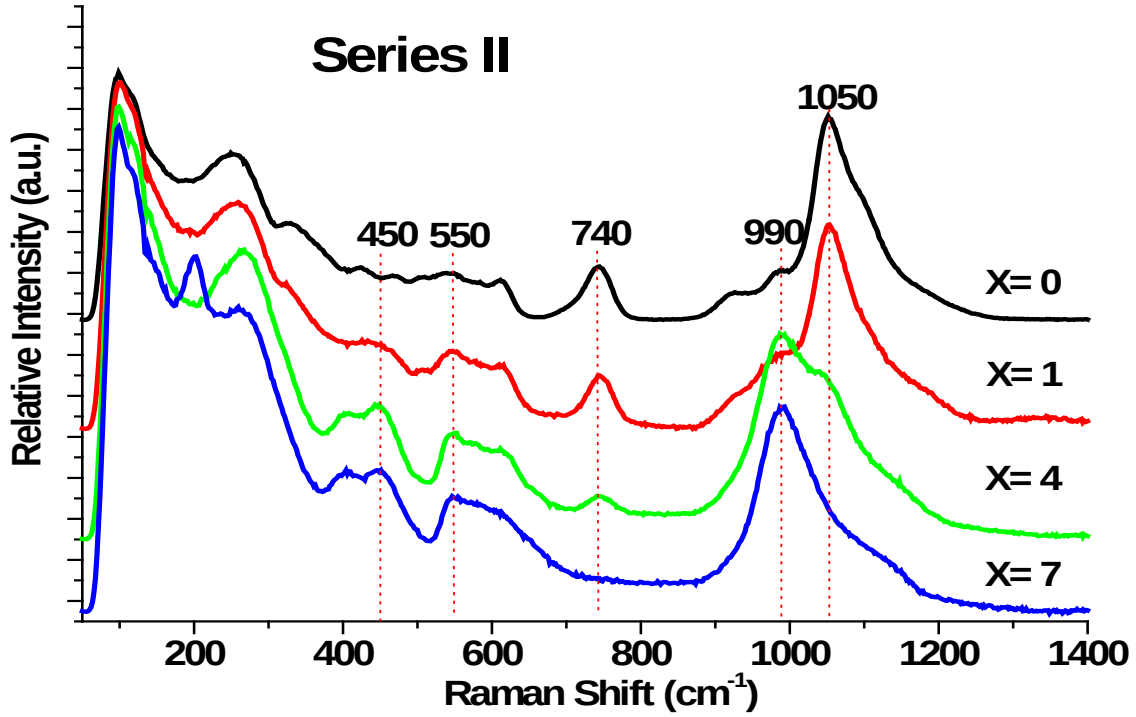

(b)

Figure 5. Raman spectra of $SnO\text{-}Ga_2O_3\text{-}P_2O_5$ (SGaP) glasses (a) in series I (b) in series II.

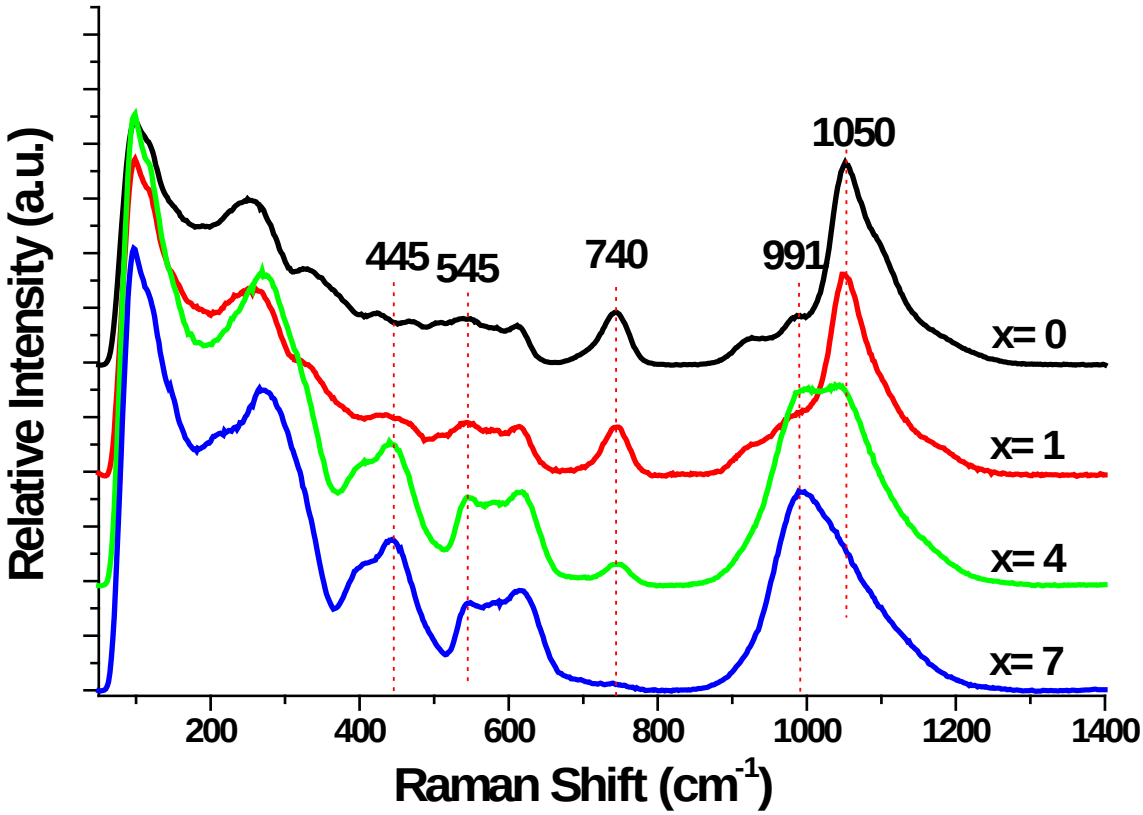

Figure 6. Raman spectra of $SnO\text{-}Sb_2O_3\text{-}P_2O_5$ (SSbP) glasses in series I.

SECTION

2. FUTURE WORK

The development of new compositions of optical glasses requires the study of the glass forming regions of new compositional systems as well as the process of making glasses. Requirements of this project are to develop the glasses which have low processing temperature, high n_d and relatively high ν_d while maintaining a good chemical durability. Sometimes, it is hard to find the right compositions for the right application and it always seems to happen in the laboratory that one property needs to be sacrificed to get the other property. For example, the glasses which have high refractive index also have high dispersion.

In this thesis, tin phosphate base glasses were former was studied and these glasses were modified with different oxides (B_2O_3, Ga_2O_3, and Sb_2O_3) to obtain desirable optical, chemical, and thermal properties. Other oxide glass formers, including the tellurite glasses, have high refractive index (larger than 2.0), wide band infrared transmittance (extending up to 6000nm), and large third order non-linear optical susceptibility [13-14]. Due to their strong nonlinear properties and an opportunity of doping with high concentrations of rare-earth elements, TeO_2 could be a good candidate for this project. However, the UV edge of tellurite glasses is about 350 nm wavelength and so it may be difficult to find colorless compositions with low dispersion. La_2O_3 or Y_2O_3 could be good candidates because they both have great ionic refractivities but also have high melting temperatures.

The studies of glass composition presented in this thesis provide a guide for future work. A number of techniques are introduced to understand the relationship between the glass structures and their properties in this study. However, the structure studies with Raman spectra are not enough to understand the phosphate glass system. The peaks and bands in the short wavenumber (cm^{-1}) regions of the Raman spectra need to be assigned to specific types of bonds. It is also necessary to understand the change of the Sn-O environment from phosphate glass system more by using NMR and Mössbauer spectroscopy [15-16]. In addition, the viscosity of these glasses has not been studied. It is important to characterize their thermo-mechanical properties due to the devitrification during the press molding operation.

APPENDIX A.

THE PROPERTIES OF GLASSES IN THE ZnO-La_2O_3-B_2O_3 SYSTEM

Glasses were prepared from the Zn-La-metaborate system, with nominal compositions: $xZn(BO_2)_2$-$(100-x)La(BO_2)_3$ (mol%) where x = 0, 10, 25, 37.5, 50. The raw materials were ZnO (Sigma Aldrich, 99.9%), La_2O_3(Research Chemicals, 99.99%), and H_3BO_3 (Alfa-Aesar, 99.8%).

All glasses were melted in alumina crucibles. Batches that produced 30g of glass were thoroughly mixed and then the crucibles were placed in a small furnace to preheat the alumina crucible at 700°C for 10 min. After heating, the crucibles were moved to the furnace and the raw materials were melted at 1000 ~ 1200°C for an hour. The crucible was removed and the melt was poured and quenched between two copper plates. The glass samples were allowed to cool in air and were annealed at 580 ~ 650°C for three hours. Weight loss was impossible to calculate because of thermal shock and the loss of pieces of the samples. Glasses were formed from each composition with no visible signs of crystallization.

Density measurements were made using the Archimedes method with de-ionized water as the suspension medium. Four samples of each glass composition were measured and the average with value and standard deviations were reported.

DTA measurements were made using a Perkin Elmer Differential Thermal Analyzer DTA 7. Bulk samples were ground and about 40mg were placed in alumina crucibles and measured in the DTA to a set point of 800 ~ 1000°C using a heating rate of 10°C/min. Onset measurements for T_g were made using the intercept method.

UV-Vis measurements were taken using a Cary 5 UV-Vis-NIR spectrophotometer. Bulk samples about 1mm thick were polished to 1µm (diamond paste). After collecting

the UV–Vis absorption data, the UV edge was defined as the wavelength at which an absorbance of 4 cm^{-1} and Figure A.1 shows the transmission of glasses.

The refractive indices of these polished samples were measured using a Metricon Refractometer (2010) at 405, 632.8, and 785 nm and an Abbe number was determined by calculating refractive indices at 656.3 nm (n_C), 589.3 nm (n_D) and 486.1 nm (n_F) after fitting the three measured refractive indices using the Cauchy dispersion equation. Table 1 lists the properties of the Zn-La-borate glasses.

Table A.1: Selected properties of the $ZnO\text{-}La_2O_3\text{-}B_2O_3$ glasses ($xZn(BO_2)_2\text{-}(100\text{-}x)*La(BO_2)_3$).

Value	**Density**	**Refrac. Index**	**Glass Trans.**	**UV-edge**	**Abbe #**
x	g/cm^3	(632.8 nm)	T_g (ºC)	nm	ν_D
0	3.676	1.6857	653	191	51.76
10	3.745	1.6935	644	201	50.93
25	3.754	1.6977	631	204	51.80
37.5	3.626	1.6772	578	208	50.49
50	3.608	1.6739	608	211	50.03

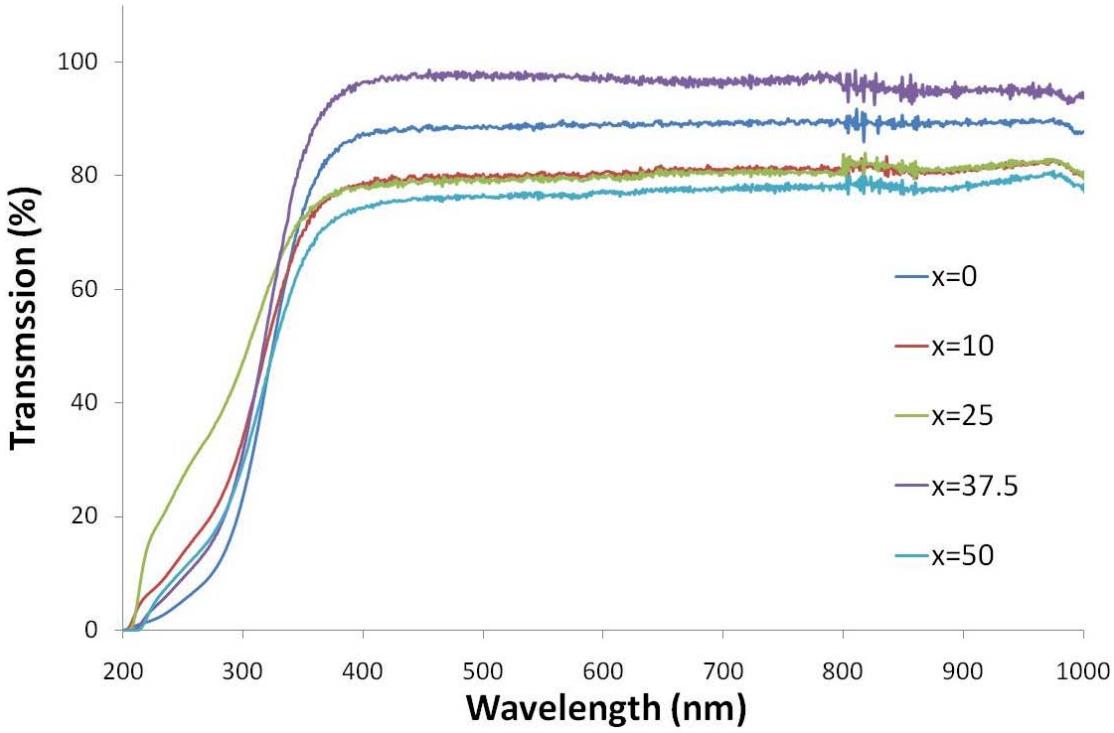

Figure A.1. Optical transmission spectra of the $xZn(BO_2)_2$-$(100-x)La(BO_2)_3$ glasses.

APPENDIX B.

THE CORROSION STUDIES OF TIN PHOSPHATE GLASSES

This appendix contains the data for the corrosion tests in aqueous environment at 40^{o}C from paper 2 and paper 3. Shown in Table B.1 and Table B.2 are wt. loss rates and these data are shown in Figure B.1 for tin borophosphate glass system and Figure B.2 for tin gallium (antimony) phosphate glass system.

Table B.1. Weight loss rate data of tin borophosphate glasses.

Hrs	0%B (g/cm^{-2})	4%B (I) (g/cm^{-2})	7%B (I) (g/cm^{-2})	10%B (I) (g/cm^{-2})	16%B (I) (g/cm^{-2})	20%B (I) (g/cm^{-2})	25%B (I) (g/cm^{-2})
0	0	0	0	0	0	0	0
1	2E-05	2E-05	0	0	6.1E-06	0	0
3	7E-05	2.7E-05	0	1.2E-05	1.2E-05	0	0
6	0.0002	3.3E-05	1.4E-05	1.2E-05	3E-05	0	1.4E-05
12	0.0004	7.4E-05	4.3E-05	3E-05	4.8E-05	1.4E-05	2.1E-05
24	0.0006	0.00011	7.2E-05	4.2E-05	5.5E-05	3.5E-05	2.8E-05
48	0.0008	0.00017	9.2E-05	4.8E-05	7.3E-05	5E-05	3.5E-05
72	0.0011	0.00017	9.6E-05	5.4E-05	7.3E-05	7.8E-05	4.9E-05
120	0.0017	0.00017	0.0001	5.4E-05	7.3E-05	9.2E-05	5.6E-05

Hrs	4%B (II) (g/cm^{-2})	7%B (II) (g/cm^{-2})	10%B (II) (g/cm^{-2})
0	0	0	0
1	2E-05	7.6E-06	0
3	4E-05	2.3E-05	1.8E-05
6	7E-05	3.8E-05	3.7E-05
12	8E-05	3.8E-05	3.7E-05
24	8E-05	5.3E-05	3.7E-05
48	7E-05	3.8E-05	3.7E-05
72	7E-05	5.3E-05	3.7E-05
120	8E-05	5.3E-05	3.7E-05

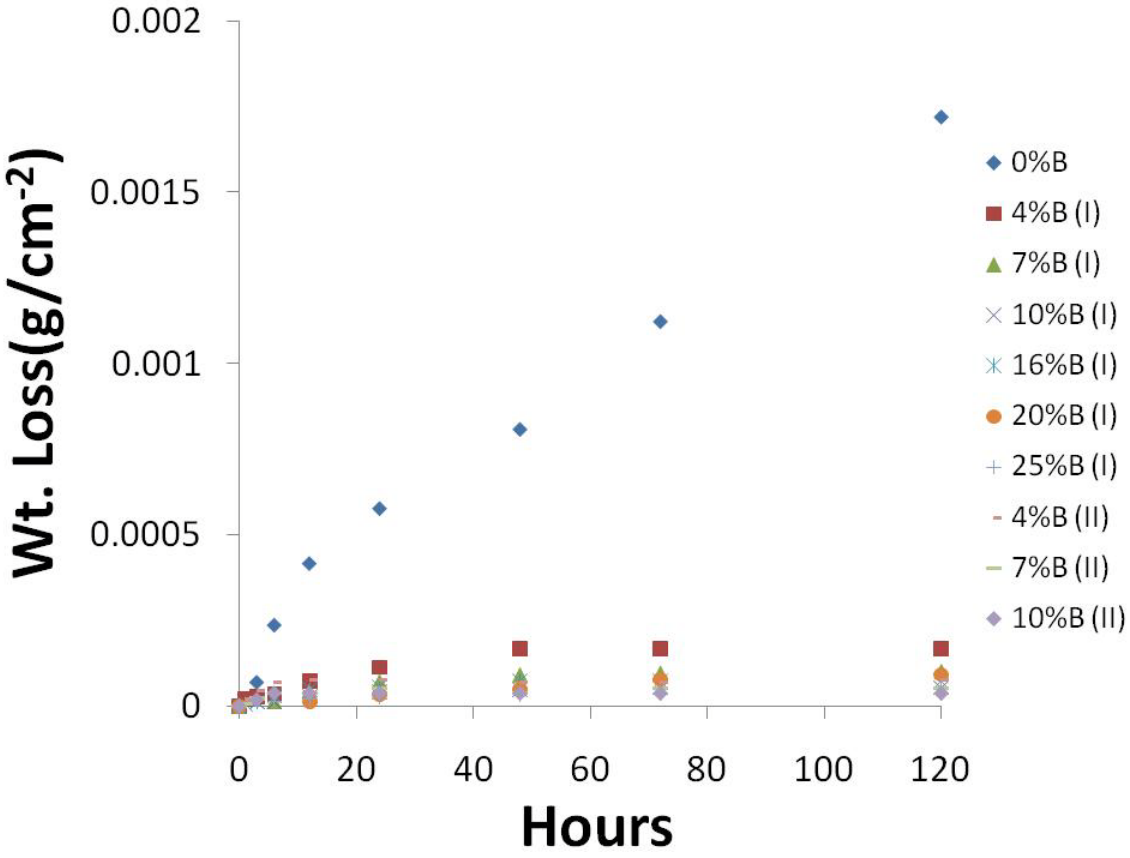

Figure B.1. The weight loss rates for tin borophosphate glasses during 120 hours of reaction in aqueous environment at 40°C.

Table B.2. Weight loss rate data of tin gallium (antimony) phosphate glasses.

Hrs	0%B (g/cm^{-2})	4%Ga (I) (g/cm^{-2})	7% Ga (I) (g/cm^{-2})	10%Ga (I) (g/cm^{-2})	4%Ga (II) (g/cm^{-2})	4%Sb (I) (g/cm^{-2})	7%Sb (I) (g/cm^{-2})
0	0	0	0	0	0	0	0
12	0.000417	2.4E-05	2.24E-05	3.05E-05	3.76E-05	2.27E-05	2.11E-05
24	0.000577	4.8E-05	2.99E-05	5.09E-05	6.77E-05	4.54E-05	3.16E-05
48	0.000808	6E-05	3.36E-05	5.7E-05	7.52E-05	4.54E-05	5.27E-05
216		7.19E-05	3.73E-05	6.1E-05	8.27E-05	4.54E-05	7.38E-05

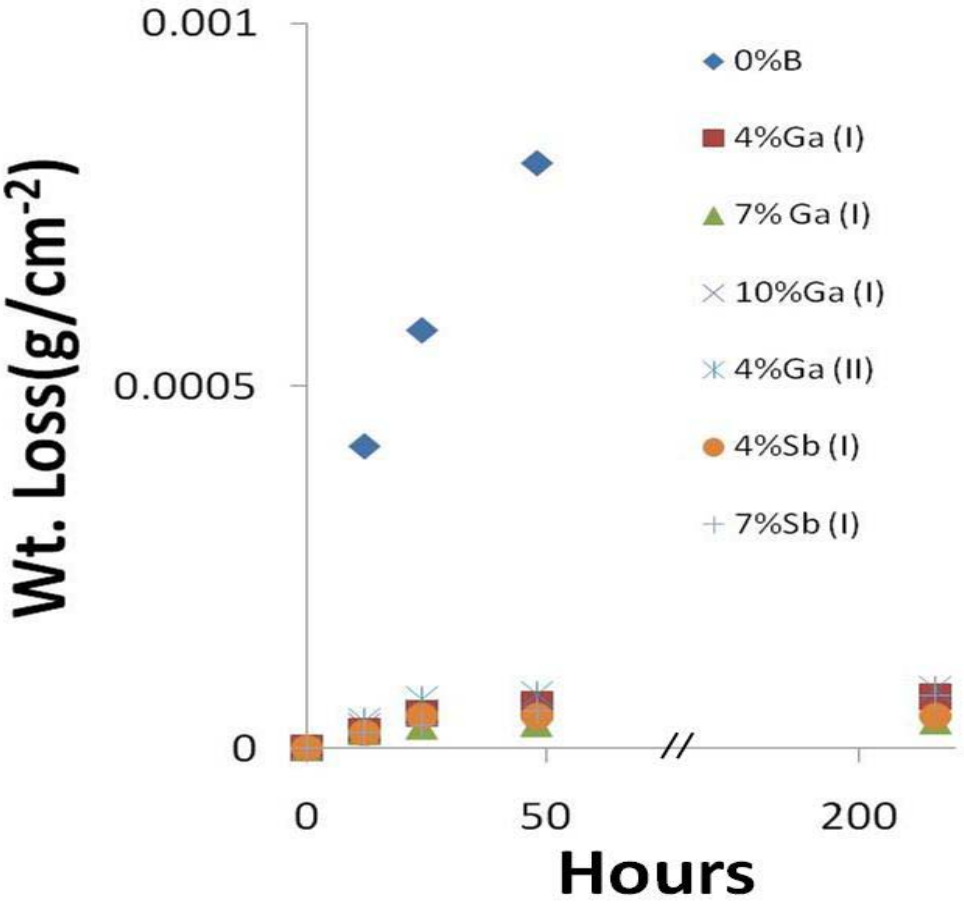

Figure B.2. The weight loss rates for tin gallium (antimony) phosphate glasses during 216 hours of reaction in aqueous environment at 40^{o}C.

BIBLIOGRAPHY

[1] I.T.R.I. IEK Report (2007).

[2] http://www.greatwalloptical.com.hk/optical.page/asphericlens.html. June 2010.

[3] http://www.tamron.com/lenses/optical.asp. June 2010.

[4] S. D. Jacobs, International Progress on Advanced Optics and Sensors, Edited by H. Ohmori and H. M. Shimizi., Universal Academy Press Inc., Tokyo, Japan, 2003. pp 3–14.

[5] R. G. Bingham, D. D. Walker, D. H. Kim, D. Brooks, R. Freeman, and D. Riley, in Proceedings of SPIE 45th Annual Meeting, the International Symposium on Optical Science and Technology, San Diego, CA, Vol. 4093, July 30–August 4, 2000, pp. 4445–8.

[6] G. A. A. Menden-Piesslinger and J. H. P. Van de Heuvel, ‘‘Precision Pressed Optical Components Made of Glass and Glass Suitable Therefore.’’ US Patent (1983) 4,391,915.

[7] R. O. Maschmeyer, C. A. Andrysick, T. W. Geyer, H. E. Meissner, C. J. Parker, and L. M. Sanford, ‘‘Precision Molded Glass Optics,’’ Appl. Opt., 22 (1983) 2413–5.

[8] Y. Kashiwagi, M. Umetani, H. Kataoka, K. Inoue, S. Nakamura, S. Morimoto, US Patent 5,759,221 (1998).

[9] K. Nakahata, K. Tsuhiya, and S.Nagahama, US Patent (2001) 6,333,282.

[10] K. Sato, US Patent (2004) 6,743,743.

[11] Y. Yamamoto, k. Tsuhiya, N. Sawanobori, and S. Nagahama, US Patent (2006) 7,141,525.

[12] http://www.us.schott.com/advanced_optics/english/our_products /materials/ data_tools /index. html. April 2008.

[13] H. Nasu, T. Uchigaki, K.Kamiya, H. Janbara and K. Kubodera, Jpn. J. Appl. Phys. 31 (1992) 3899.

[14] S. H. Kim, T. Yoko, and S. Sakka, J. Am. Cerm. Soc. 76 (1993) 2486.

[15] D. Holland, S.P. Howes, M.E. Smith, and A.C. Hannon, J. Phys.:Condens. Matter 14 (2002) 13609.

[16] E. Bekaert, L. Montagne, L. Delevoye, G. Palavit, and B. Revel, C.R. Chimie 7 (2004) 377.

VITA

Jong Wook Lim is the son of Sam Rang Lim and Hwa Lee and was born on August 2, 1972 in Seoul, Korea. He attended Young Dong High School, Seoul, Korea before attending Coe College in Cedar Rapids, Iowa and earned a B.S. with a major in Physics while also minor in Mathematics in May of 2000. He then began his graduate work in June of 2000 at Lehigh University and received an M.S. degree in Materials Science and Engineering in January of 2004. After finishing M.S degree, he went to Bolivia and became a facility manager and processing engineer in the zipper factory until December of 2007. He began his M.S. program in January of 2008 at the Missouri University Science and Technology in Rolla in Ceramic Engineering, graduating in December of 2010.